



Virginia Commonwealth University
VCU Scholars Compass

Theses and Dissertations

Graduate School

2012

BIOCHEMICAL ACTIONS OF A NOVEL CIS-TERPENONE

Lin Zhang
Virginia Commonwealth University

Follow this and additional works at: <https://scholarscompass.vcu.edu/etd>

 Part of the [Chemistry Commons](#)

© The Author

Downloaded from

<https://scholarscompass.vcu.edu/etd/414>

This Dissertation is brought to you for free and open access by the Graduate School at VCU Scholars Compass. It has been accepted for inclusion in Theses and Dissertations by an authorized administrator of VCU Scholars Compass. For more information, please contact libcompass@vcu.edu.

Lin Zhang, 2012
All Rights Reserved

BIOCHEMICAL ACTIONS OF A NOVEL CIS-TERPENONE

A dissertation submitted in partial fulfillment of the requirements for the degree of
Doctor of Philosophy at Virginia Commonwealth University.

by

Lin Zhang

Master of Chemistry, Nankai University, 1999

Director: Qibing Zhou, Ph.D

ASSISTANT PROFESSOR, DEPARTMENT OF CHEMISTRY

Virginia Commonwealth University
Richmond, Virginia
June, 2012

Acknowledgement

First and foremost I want to thank my dissertation advisor Dr. Qibing Zhou. Without him, this dissertation would not have been possible. I appreciate all his contributions of time, ideas, and funding to my Ph.D. work. I thank him for his insights and suggestions that helped to shape my research skills.

I owe my deepest gratitude to Dr. Jennifer K. Stewart, not only for helping me with biology part of my dissertation, but also for her patience and encouragement that carried me on through my difficult times.

I would like to thank the rest of my committee members: Dr. Nicholas Farrell, Dr. Scott Gronert and Dr. Suzanne Ruder. Their valuable feedback helped me to improve the dissertation in many ways. I also thank Dr. Sarah Rutan, who advised and helped me during the tough time in my Ph.D. pursuit.

I thank the Department of Chemistry for providing me financial support. I also thank my group members: Miguel Zuniga and Ting Xu. I enjoyed all the discussions we had on various topics.

Last but not least, I would like to thank my parents, Yunliang Zhang and Yuhua Zhao and my sister Ping for always being there when I needed them, and for supporting me through all these years. I also thank my wife, Yun Zhu for her love, faithful support and encouragement which are most important to me throughout the years.

TABLE OF CONTENTS

Acknowledgements	iii
List of Figures	vi
List of Schemes	viii
List of Abbreviations	x
Abstract	xii
Chapter	
1 Introduction	1
1.1 Natural terpenes	1
1.2 Quinone methides	2
1.3 Target compound and analogs	5
2 Aflatoxins and CYP 450	10
2.1 Aflatoxins	10
2.2 Cytochrome P450s	14
2.3 Chemoprevention compounds against AFB1	19
3 Chemoprotective Actions of Hydroxy-Cis-Terpenone (HCT) Against Aflatoxin	22
3.1 Actions of HCT on liver cell viability	22
3.2 Actions of Cis-Terpenones on Cytochrome P450 (CYP450)	36
3.3 Liver Microsomes and P450 3A4 Studies with HCT	38
4 Actions of HCT on AFB1 Accumulation in HepG2 Cells	43
4.1 Cellular Uptake and Efflux of AFB1	43
4.2 Results and Discussion	47
5 Preliminary Studies of Other biological actions of HCT and OHCT	63
5.1 Anti-inflammatory Effects of HCT on Macrophages	63
5.2 Biological Actions of OHCT	70
5.3 Effects of OHCT on Cellular MDR1-mediated Efflux of AFB1 and Estrone Sulfate	72
5.4 Preliminary studies with H69AR cells expressing MRP1	76

References.....	79
-----------------	----

List of Figures

	Page
Figure 1.1: The unique 3-D conformation of HCT versus that of estradiol	9
Figure 2.1: Intercalation of AFB1 into DNA.....	13
Figure 2.2: Human CYP450 3A4 ribbon detail	15
Figure 2.3: Contribution of major human P450s to the Phase I metabolism of all drugs currently marketed	19
Figure 3.1: 2D NOESY NMR Spectrum of <i>cis</i> -terpenone compound.....	34
Figure 3.2: Chemo-protection with <i>cis</i> -terpenones against AFB1-induced cytotoxicity	35
Figure 3.3: Inhibition of TCDD-induced P450 1A/B activity with <i>cis</i> -terpenones.....	37
Figure 3.4: Inhibitory effects of HCT and OHCT on the activity of purified P450 3A4	40
Figure 3.5: Inhibitory effects of HCT and OHCT on the activity of purified P450 3A4	41
Figure 3.6: Chemo-protection with OHCT and ketoconazole against AFB1-induced cytotoxicity	41
Figure 4.1: Time-dependent accumulation of [3H]-AFB1 by HepG2 cells	48
Figure 4.2: Concentration dependent inhibition of [3H]-AFB1 accumulation with HCT....	49
Figure 4.3: Concentration dependent inhibition of [3H]-AFB1 accumulation with AFB1 ..	50
Figure 4.4: Effects of 3 mM sodium azide (NaN ₃) on [3H]-AFB1 accumulation	51
Figure 4.5: Effects of maximal concentrations of inhibitors and substrates on [3H]-AFB1 accumulation in HepG2 cells	52
Figure 4.6: Effects of ions and N-ethylmaleimide on [3H]-AFB1 accumulation in HepG2 cells	53
Figure 4.7: Inhibition of [3H]-AFB1 accumulation with probenecid in HepG2 cells.....	54
Figure 4.8: Inhibition of [3H]-AFB1 accumulation with verapamil in HepG2 cells.....	54

Figure 4.9: Inhibition of [3H]-AFB1 accumulation with 17- β -Estradiol in HepG2 cells ...	55
Figure 4.10: HCT, verapamil and unlabeled AFB1 decreased binding of [3H]-AFB1 to liver microsomes.....	57
Figure 4.11: 17- β -estradiol binding of [3H]-AFB1 to human liver microsomes.....	58
Figure 4.12: Effects of pH on accumulation of [3H]-AFB1 in Hep G2 cells.....	60
Figure 4.13: Accumulation of ([3H]-ES in wild type (WT) CHO cells and CHO cells expressing OATPB	61
Figure 4.14: Effects of HCT on accumulation of ([3H]-ES in wild type (WT) CHO cells and CHO cells expressing OATPB.....	62
Figure 5.1: Image of human Interleukin-6.....	64
Figure 5.2: Image of human TNF α	65
Figure 5.3: Effects of HCT on LPS-stimulated release of IL-6 and TNF α by RAW264.7 cells	68
Figure 5.4: Effects of LPS with HCT on release by RAW264.7 cells.....	69
Figure 5.5: Effects of OHCT on [3H]-AFB1 accumulation	74
Figure 5.6: Effects of OHCT on [3H]-ES accumulation	75
Figure 5.7: Time-dependent accumulation of [3H]-ES by H69AR cells in the presence of the MRP1 inhibitor MK571	78

List of Schemes

	Page
Scheme 1.1: Structure of Calotropin, a cardenolide	2
Scheme 1.2: Formation of Quinone Methide.....	2
Scheme 1.3: Quinone Methide nucleophilic addition.....	3
Scheme 1.4: Structure of Vitamin E	3
Scheme 1.5: Structure of Celastrol	4
Scheme 1.6: Examples of bioactive natural terpene products	5
Scheme 1.7: The oxidative conversion of a cascade of analogs with Cu^{2+} and $\text{HSCH}_2\text{CH}_2\text{OH}$	6
Scheme 1.8: Metabolic pathways for Trans-terpenone.....	7
Scheme 1.9: Structure of cis-terpenone (HCT) analogs	8
Scheme 2.1: Structures of Aflatoxins	11
Scheme 2.2: Metabolism of AFB1 by CYP450 and bonding with DNA	12
Scheme 2.3: Kinetics of AFB1 exo-8,9-epoxide interaction with DNA	13
Scheme 2.4: Aflatoxin B1 oxidation products.....	14
Scheme 2.5: Consensus catalytic cycle for oxygen activation and transfer by cytochrome P450	16
Scheme 2.6: Possible pathway for oxygen-atom transfer from the active ferryl species to form the alcohol.....	17
Scheme 2.7: Effect of oltipraz on the metabolism of aflatoxin B ₁	20
Scheme 3.1: Structure of cis-terpenone analogs.....	22
Scheme 3.2: Synthesis of cis-Terpenones 1-3	27

Scheme 3.3: Detailed synthesis mechanism of cis-Terpenones.....	28-29
Scheme 3.4: MTT Reduction.....	30
Scheme 3.5: 7-ethoxyresorufin deethylation reaction	32
Scheme 3.6: OHCT as the Spontaneous Oxidation Product of HCT	38
Scheme 5.1: Structure of Chloroquine.....	70
Table 5.1: OHCT (nM) inhibits growth of <i>P. falciparum</i> gametocytes.....	71
Scheme 5.2: Structure of Estrone 3-sulfate potassium salt.....	72

LIST OF Abbreviations

^3H	Tritium
AFB1	Aflatoxin B1
CHO	Chinese hamster ovarian cells
CYP450	Cytochrome P450
DMF	N, N'-Dimethylformamide
DMSO	Dimethyl sulfoxide
DTT	Diothiothrietol
EROD	Ethoxyresorufin-O-deethylase
ES	Estrone Sulfate
FBS	Heat-inactivated fetal bovine serum
FCCP	Carbamyl cyanide 4-(trifluoromethoxy) phenylhydrazone
GSH	Glutathione
GSHE	Gluthione ester
GSTs	Glutathione S-transferases
HCT	3-hydroxy-cis-terpenone
HepG2	Human hepatocellular carcinoma cells
IL-6	Interleukin-6
LPS	Lipopolysaccharide
MDR1	Multi-drug resistant efflux transporter
MEM	Minimum Essential Eagle medium
MRP1	Multi-drug resistant protein-1

MTT	3-(4,5-Dimethylthiazol-2-yl)-2,5-diphenyltetrazolium bromide
NEM	N-ethyl maleimide
OAT	Organic anion transporters
OCT	Organic cation transporters
OHCT	Oxidized 3-hydroxy-cis-terpenone
PAH	Para-amino-hippuric acid
PBS	Phosphate buffered saline
SH	Sucrose/Hepes
TCDD	2,3,7,8-tetrachlorodibenzo-p-dioxin
TNF α	Tumor necrosis factor α
TPQMs	Triterpene quinone methides

Abstract

BIOCHEMICAL ACTIONS OF A NOVEL CIS-TERPENONE

By Lin Zhang, Ph.D.

A dissertation submitted in partial fulfillment of the requirements for the degree of
Doctor of Philosophy at Virginia Commonwealth University.

Virginia Commonwealth University, 2012

Director: Qibing Zhou, Ph.D
Assistant Professor Department of Chemistry

Quinone methides are reactive species due to their electrophilicity, and natural quinone methide analogs have broad biological activities. Based on known actions of cytochrome P450 enzymes, we hypothesized that trans-terpenones can be metabolized in cells to form a cascade of metabolite products, which may be biologically active due to the generation of quinone and quinone methide reactive intermediates. Therefore, 3-hydroxy-cis-terpenone (HCT) and analogs were designed and synthesized in our lab to investigate this hypothesis.

As a first step in testing this hypothesis, we examined effects of cis-terpenones on the viability of HepG2 cells exposed to aflatoxin B1 (AFB1). Cis-terpenones combined

with AFB1 in HepG2 cells increased cell viability suggesting chemopreventive effects against AFB1. Further study revealed a mechanism for this effect: HCT and oxidized HCT (OHCT) inhibited activity of P450 1A/B, which metabolizes AFB1 to toxic metabolites, and thereby protected cells against AFB1 induced cytotoxicity.

Additional studies demonstrated that HCT inhibits accumulation of tritium-labeled AFB1 in HepG2 cells. To investigate the mechanism of this effect we first determined whether specific transporters affect the accumulation of AFB1 in HepG2 cells. Effects on AFB1 accumulation by pH, selected ions, inhibitors or competitive substrates of organic cation transporters (OCT), organic anion transporters (OAT/OATP), and multi-drug-resistant efflux transporters eliminated effects of major groups of these transporters on AFB1 accumulation. The data indicated one or more unidentified proton dependent transport mechanism(s) modulate cellular accumulation of AFB1 and further demonstrated HCT inhibits accumulation of AFB1 in cells by decreasing AFB1 binding to intracellular proteins.

Based on its potential chemoprotective actions, other biological actions of HCT were screened. Based on evidence that terpenes modulate immune cell production of cytokines, we examined effects of HCT on production of interleukin-6 (IL-6) and tumor necrosis factor- α (TNF α) by cultured macrophages. HCT reduced lipopolysaccharide-stimulated release of IL-6 and TNF α . MES-SA/DX5 cells that over-express the efflux transporter MDR1 were used to examine effects of OHCT on accumulation of the MDR1 substrate estrone-sulfate and to verify that MDR1 does not transport unconjugated AFB1.

OHCT at a high concentration (120 μ M) reduced cellular accumulation of estrone sulfate suggesting enhanced MDR1-mediated efflux

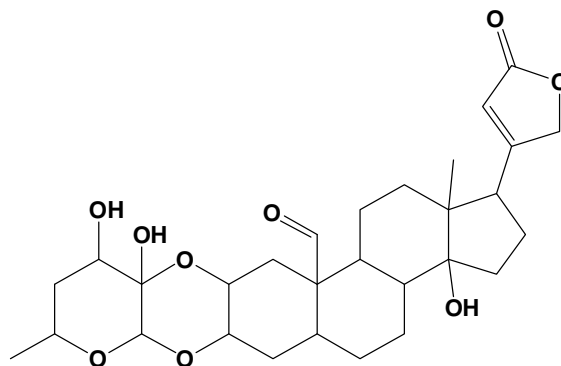
Chapter 1

Introduction

1.1 Natural terpenes

Approximately 25,000 natural terpenes have been reported,¹ however, most of these compounds exhibit no apparent functional actions in growth and development and were treated initially as metabolite waste. This traditional view remained until the 1970s, and very few of these compounds were fully investigated. Starting in the 1970s, many terpenes were discovered to have antibacterial and antifungal activity, which led to numerous studies on these natural products.²

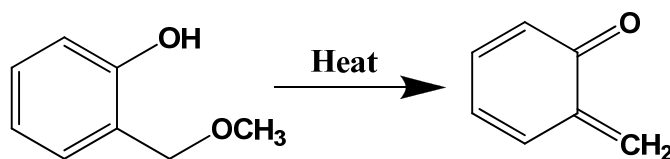
Many animals, plants and insects can produce terpenes and use them mostly as defense weapons. For example, Milkweed *Asclepias curassavica* contains cardenolides in its latex canals, which are toxic to insects. When *Trichoplusia ni* were fed on Milkweed *Asclepias curassavica*, they suffered severe spasms and became immobilized (Scheme 1.1).³ Another example is termites which can produce the monoterpene-, sesquiterpene- and diterpene mixture, which the insects use as protective substances.⁴



Scheme 1.1 Structure of Calotropin, a cardenolide (J. Gershenzon, et. al., 2007)

1.2 Quinone methides

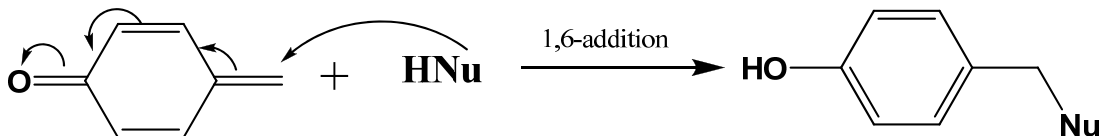
Among approximate 25,000 of terpene family members, triterpene quinone methides (TPQMs) have attracted our attention particularly because of their quinone methide moiety. In 1907, K. Fries first suggested a quinone methide intermediate,⁵ and in 1963 Gardner identified the intermediate by the pyrolysis of o-methoxymethylphenol using spectroscopical methods (Scheme 1.2).⁶



Scheme 1.2 Formation of Quinone Methide (Gardner et. al., 1963)

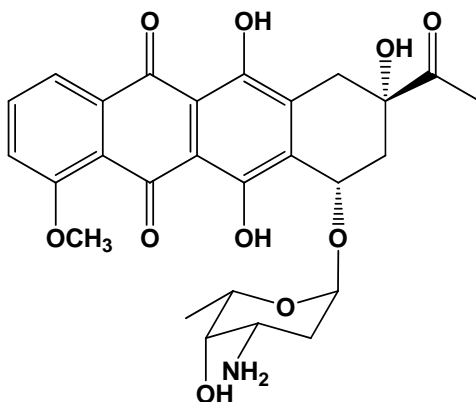
Quinone methides are very reactive species due to their electrophilicity.

Nucleophiles can attack the methylene group and form an aromatic phenol (Scheme 1.3).



Scheme 1.3 Quinone Methide nucleophilic addition (V. D. Water, et. al., 2002)

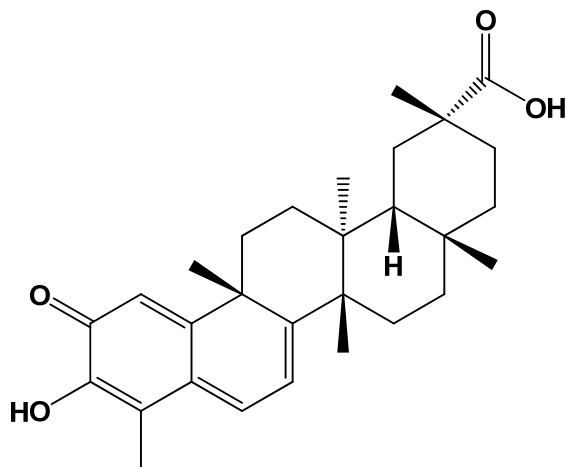
Quinone methides are the intermediates that often exist in nature. Natural quinone methide analogs can be therapeutic agents or antibiotic agents. For example, both Vitamin E's therapeutic effects and anthracycline's antibiotic action are due to formation of quinone methide species (Scheme 1.4).⁷



Scheme 1.4 Structure of Vitamin E (Van De Water, et. al., 2002)

A second example of quinone methide is the potent natural terpene product Celastrol (Scheme 1.5) that is extracted from the root bark of “Thunder of God Vine”, which has been used as traditional Chinese medicine for thousands of years to treat inflammatory conditions.⁸ It has been reported that Celastrol can induce leukemia cell apoptosis and inhibit the chymotrypsin-like activity of a purified 20S proteasome (IC_{50} =

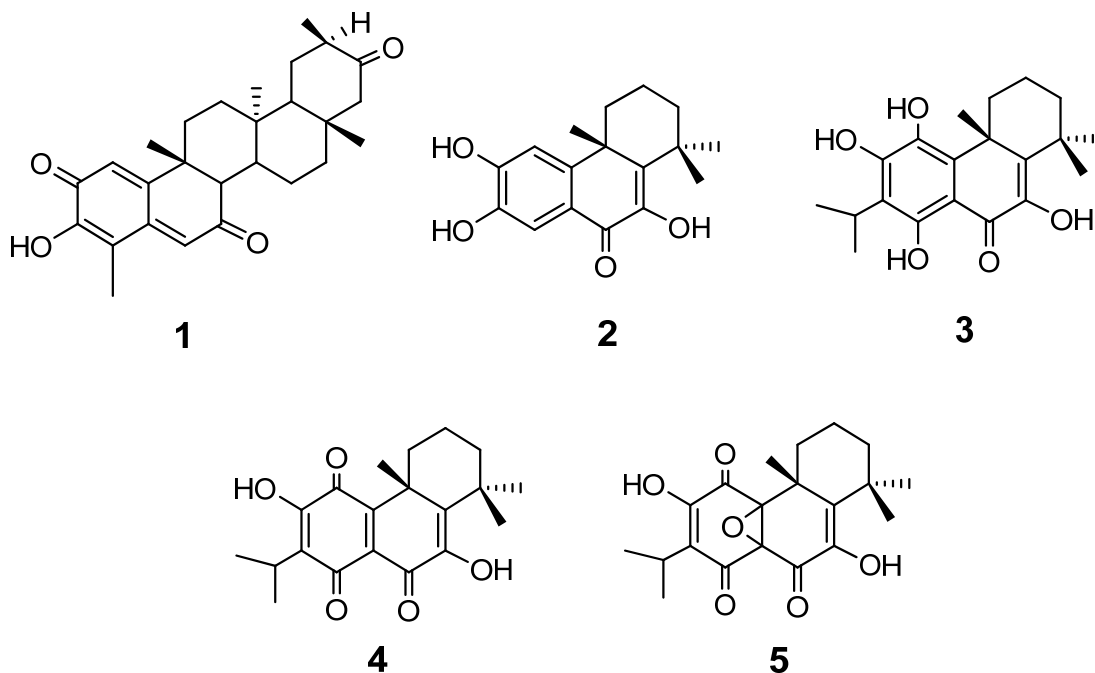
2.5 $\mu\text{mol/L}$) and human prostate cancer cellular 26S proteasome (at 1-5 $\mu\text{mol/L}$). The celastrol treatment of nude mice with PC-3 tumor resulted in great inhibition (65-93 %) of tumor growth by inhibition of proteasome activity, which implied that Celastrol may be used as potential antitumor drug.



Scheme 1.5 Structure of Celastrol, a potential chemopreventive compound
(Yang, H. J., et. al., 2006)

Another example of quinone methide is Tingenone (#1, Scheme 1.6), which is a triterpene quinone methide that exhibits 50% inhibition of growth at concentrations of 2.5-5 $\mu\text{g/mL}$ against the P-388 lymphoid neoplasm, the A-549 human lung cancer, HT-29 colon carcinoma, and MEL-28 human melanoma cell lines.⁹ Celephanol (#2) can inhibit the production of NF- κ B and nitric oxide at 18 and 32 μM , respectively.¹⁰ Coleon U (#3) exhibits 50% inhibition of cell growth at 3-6 μM against the MCF-7 breast adenocarcinoma, NCI-H460 non-small cell lung cancer, SF-269 CNS cancer, TK-10 renal cancer, and UACC-62 melanoma.¹¹ Coleon U quinone (#4) and its epoxide

derivative (#5) inhibit cell growth by 50% at concentrations of 3 and 14 $\mu\text{g/mL}$ against leukemia cells, respectively.¹²

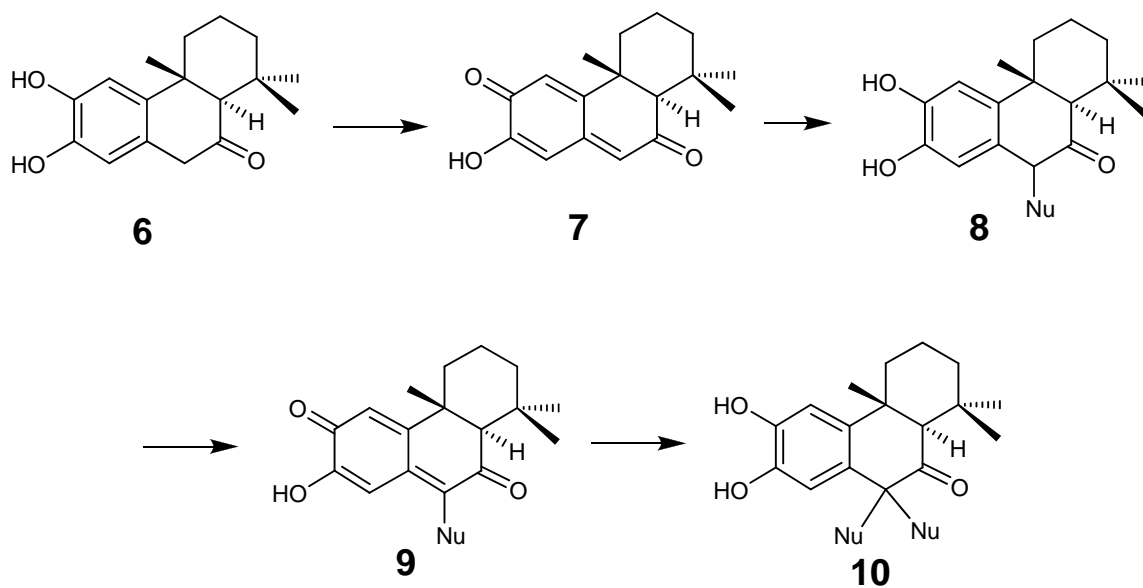


Scheme 1.6 Examples of bioactive natural terpene products (oxidation states increasing from that of tingenone 1 to epoxide 5)

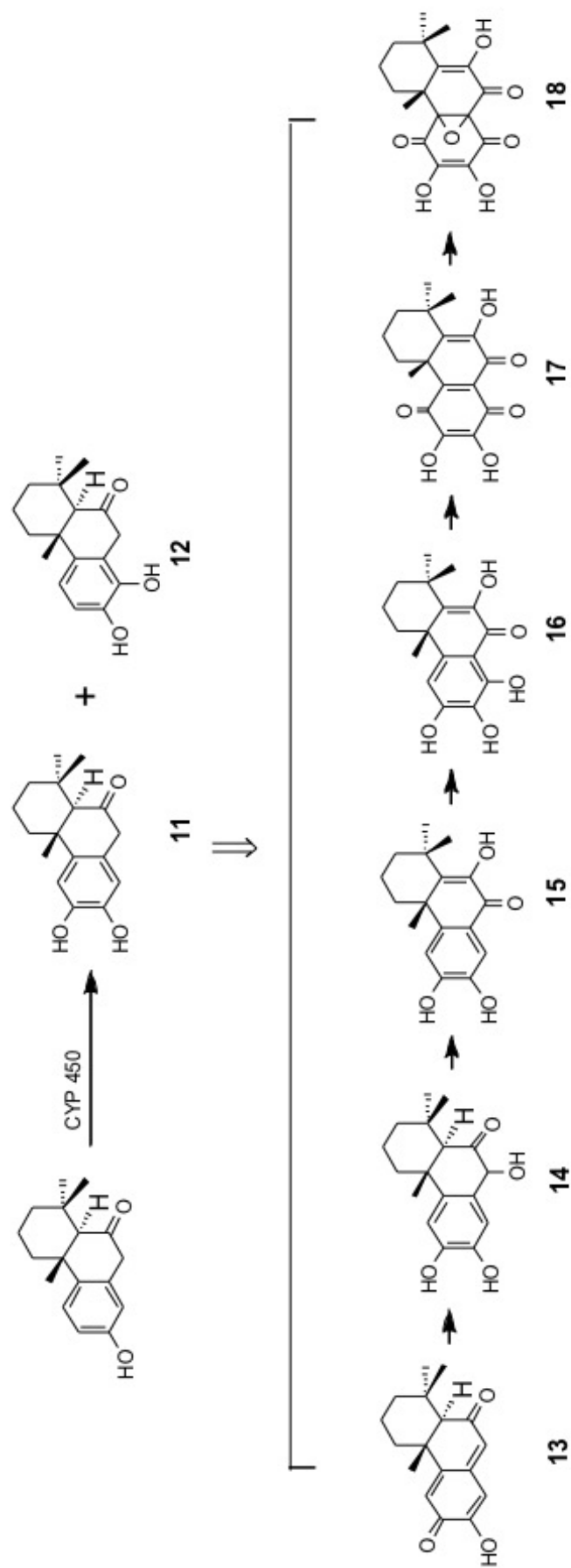
1.3 Target compound and analogs

By carefully examining above (compound 1-5) structures, if ignoring the different substitution groups, Dr. Zhou and Miguel Zuniga found that terpenes can be chemically oxidized from one parent compound by simple oxidation and addition of a hydroxyl group to form a cascade of analogs from Tingenone to Coleon U quinone epoxide derivative. In our previous papers, it was demonstrated that this conversion from

compound (#6) to compound (#7-10) is possible in solution with the presence of Cu^{2+} and $\text{HSCH}_2\text{CH}_2\text{OH}$.¹³⁻¹⁴

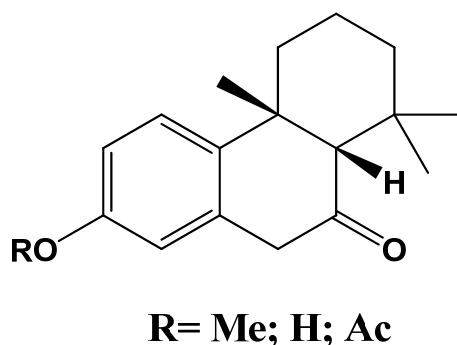


Scheme 1.7 The oxidative conversion of a cascade of analogs with Cu^{2+} and $\text{HSCH}_2\text{CH}_2\text{OH}$



Scheme 1.8 Metabolic pathways for Trans-terpenone. (Q. Zhou, unpublished)

Based on the well known actions of cytochrome P450 enzymes, Dr. Zhou hypothesized that the trans-isomers can be metabolized in cells to form a cascade of metabolite products (Scheme 1.8). It may be first hydrolyzed to a mixture of two catechol isomers 11 and 12 via CYP 450. Compound 11 shown above may be oxidized to a cascade of bioactive metabolite compounds (13-18). These compounds were hypothesized to be potentially cytotoxic due to the generation of quinone methide reactive intermediates, as well as reactive oxygen species.



Scheme 1.9 Structure of cis-terpenone (HCT) analogs

Based on these findings, 3-hydroxy-cis-terpenone (HCT) and analogs (Scheme 1.9) were designed and synthesized in our lab.¹³ Based on the metabolism of estradiol, Dr. Zhou predicted that the cis-terpenones would be hydroxylated and oxidized in liver cells. Because the predicted metabolite partially resembles resveratrol, a compound known to inhibit cytochrome P450 1A/B activity, we predicted that HCT also would inhibit one or more CYP450 enzymes.

Although the structure of HCT is similar to that of estradiol, it has a cis conformation which is different from related structures, such as our previous compound 6 and estradiol. We proposed that its unique bent conformation (Figure 1.1) would prevent the formation of HCT-DNA adducts; therefore, we expected that this compound would have no significant carcinogenic activity and may have great potential to be chemoprevention agent.¹⁵

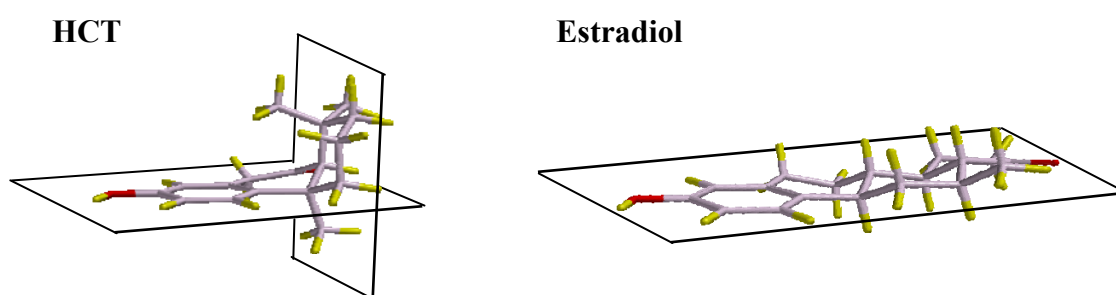


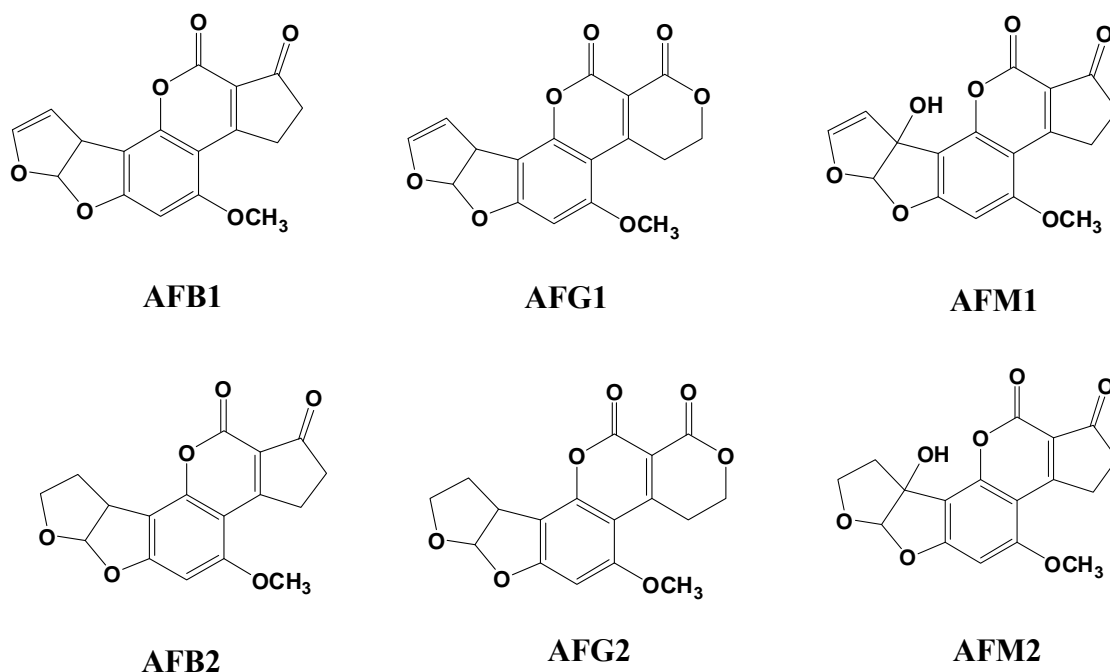
Figure 1.1 The unique 3-D conformation of HCT versus that of estradiol. The bent shape of HCT is hypothesized to prevent potential carcinogenic activity. (Q. Zhou, unpublished)

Chapter 2

Aflatoxins and CYP 450

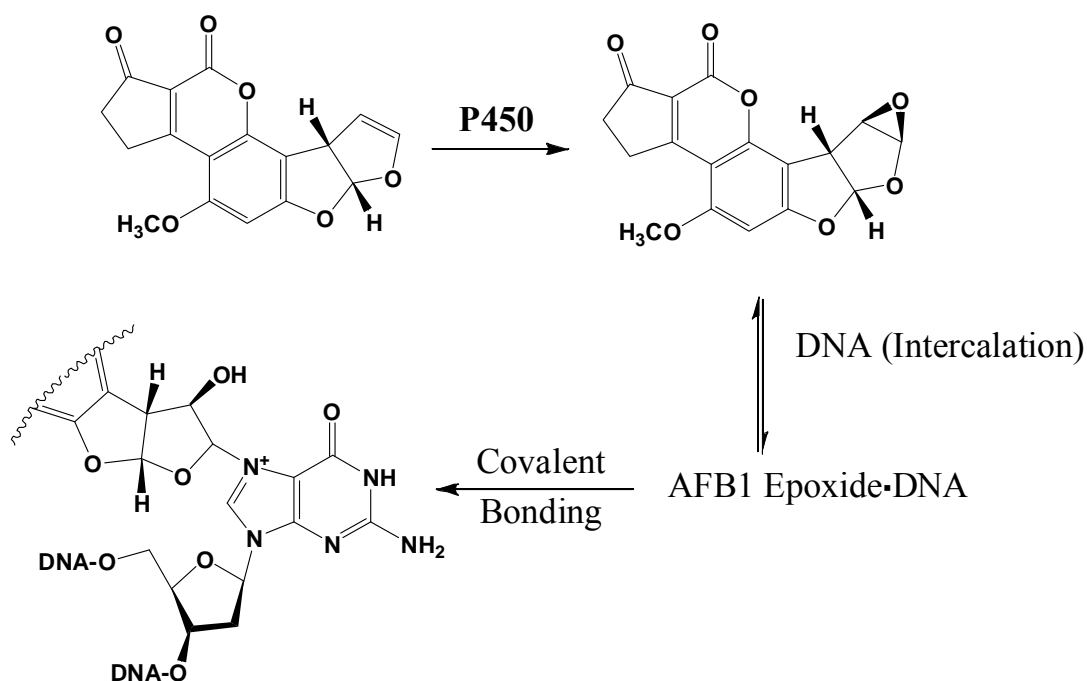
2.1 Aflatoxins

Aflatoxins probably are among the most known and researched mycotoxins. These toxins are responsible for up to 25 % of the world's crop damage.¹⁶ They were first detected and identified in 1960 as the cause of "Turkey X disease".^{17,18} Since then, aflatoxins have been studied worldwide because of their cytotoxicity to human liver cells and, more importantly, because of the possibility of causing hepatocellular carcinoma. Aflatoxins are secondary metabolites produced by a fungus *Aspergillus flavus* and are usually found in contaminated crops such as corn, peanut and cottonseed, as well as milk. There are four major aflatoxins: Aflatoxin B₁/2 and G₁/2, plus two additional hydroxylated metabolic products, M₁ and M₂ (Scheme 2.1), which were first discovered in the milk of dairy cows fed with aflatoxin contaminated diet.



Scheme 2.1 Structures of Aflatoxins

Among Aflatoxin family members, Aflatoxin B1 (AFB1) is the most toxic one. In 1988, it was listed as a human carcinogen by the International Agency for Research on Cancer (IARC, part of the World Health Organization), based on studies in Africa and Asia showing a positive association between AFB1 and liver cell cancer.¹⁹ The biological metabolism of AFB1 is already well established. Bioactivation of AFB1 goes through metabolic activation by cytochrome P450 (CYP450) to two metabolic products: AFB1 exo-8,9-epoxide and endo-8,9-epoxide. AFB1 exo-8,9-epoxide then reacts with DNA to form a covalent bonding molecular complex that causes DNA damage.²⁰⁻²³ (Scheme 2.2)

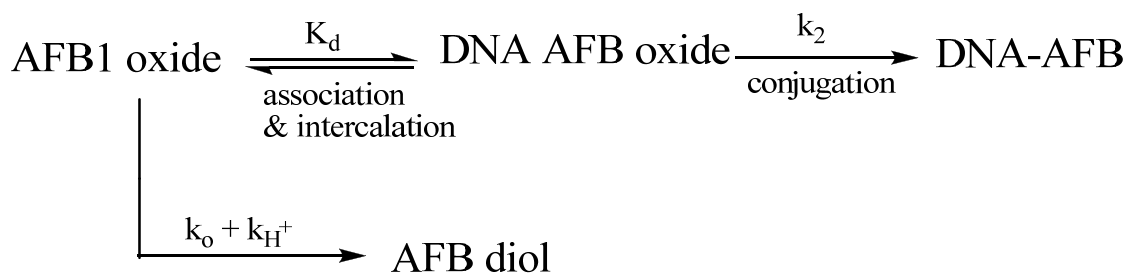


Scheme 2.2 Metabolism of AFB₁ by CYP450 and bonding with DNA

In humans, P450 1A2 and 3A4 activity account for most of the enzymatic metabolism of AFB₁. Although P450 1A2 is a more efficient catalyst,²⁴ P450 3A4 appears to be the dominant P450 involved in the formation of the exo-epoxide, due to a larger amount of 3A4 in human liver cells compared to 1A2. P450 1A2 can oxidize AFB₁ to AFM₁, AFQ₁, as well as the endo- and exo-epoxide, while P450 3A4 oxidizes AFB₁ to AFQ₁ and the exo-epoxide.²⁵

Only the exo-epoxide is genotoxic because the S_N2 reaction between the epoxide and DNA requires the guanyl N7 atom attack from the back side of the molecule

(Scheme 2.3).²⁶ The exo-epoxide reacts with DNA leading to >98% yield with $K_d = 1.4$ mM for binding/dissociation and $k_{cat} = 35 \text{ s}^{-1}$ for a rate constant yielding product.²⁷



Scheme 2.3 Kinetics of AFB1 exo-8,9-epoxide interaction with DNA

(Johnson, et. al., 1997)

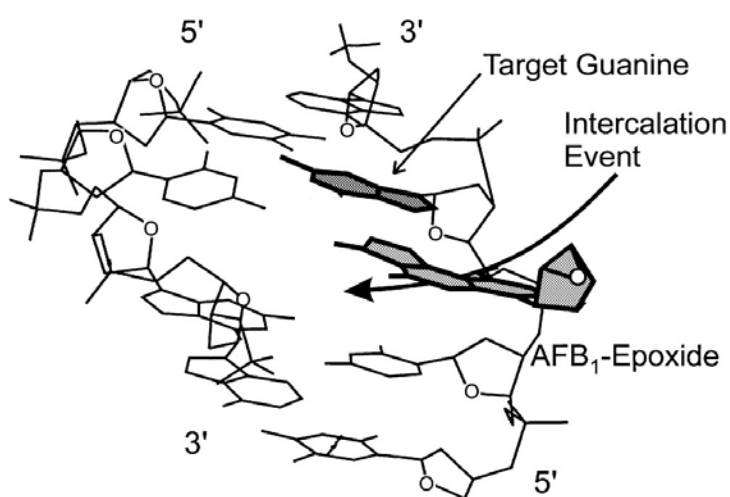
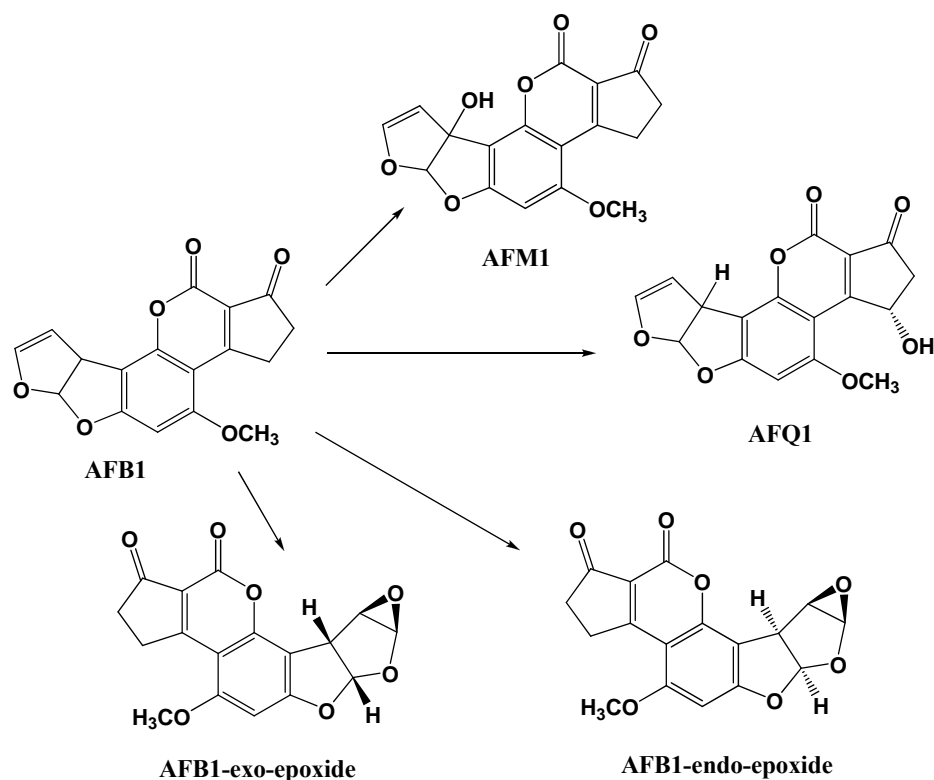


Figure 2.1 Intercalation of AFB1 into DNA (Smela et. al., 2001)

2.2 Cytochrome P450s

Since the toxic AFB1 exo-8,9-epoxide metabolite is formed from AFB1 by cytochrome P450 (CYP450), we first reviewed the function of CYP450 and decided to investigate whether cis-terpenones have the potential to block the activity of CYP450.



Scheme 2.4 Aflatoxin B1 oxidation products (Guengerich, et. al., 1998)

The cytochrome P450s (CYP450) are a series of enzymes, which are very important in human and animal's biological cell function. CYP450s have been a focus for more than three decades in biochemistry, toxicology and pharmacology because of their unique enzyme catalysis properties.²⁸ These properties are associated with their unique

folded structures.²⁹⁻³⁰ Until now, no other molecules have been found to have the same folding as CYP450. Thus, the actions and properties of CYP450, such as activation of molecular oxygen, binding of redox partners and the stereochemistry must be based on their structures.

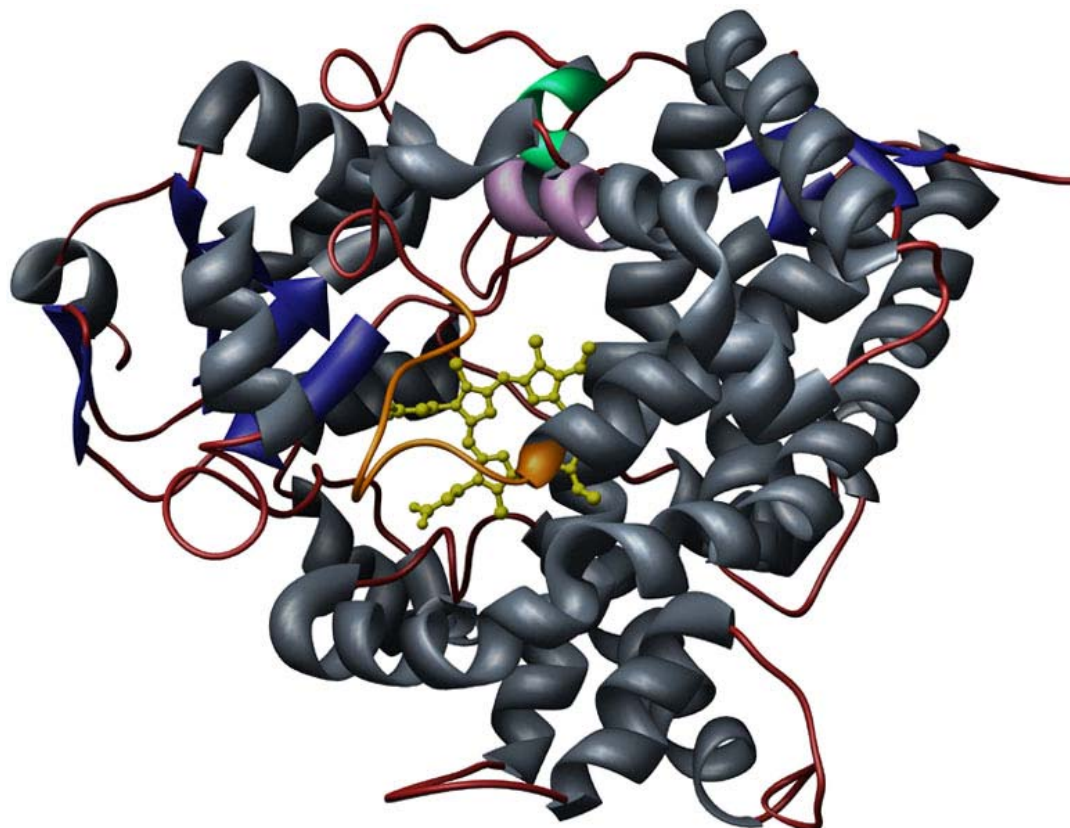


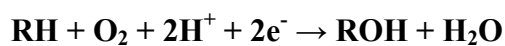
Figure 2.2 Human CYP450 3A4, [1TQN, *Homo sapiens*] ribbon detail. Color key: helix structures, gray; strand structures, blue; PERF consensus, green; K-helix concensus, purple; heme-binding consensus, orange; heme ligand, yellow.

(<http://www.p450.kvl.dk/gallery/CYP3A4.jpg> based on the work for the following paper: Paquette SM, Bak S, Feyereisen R. DNA and Cell Biology (2000) 19 (5):307-17)

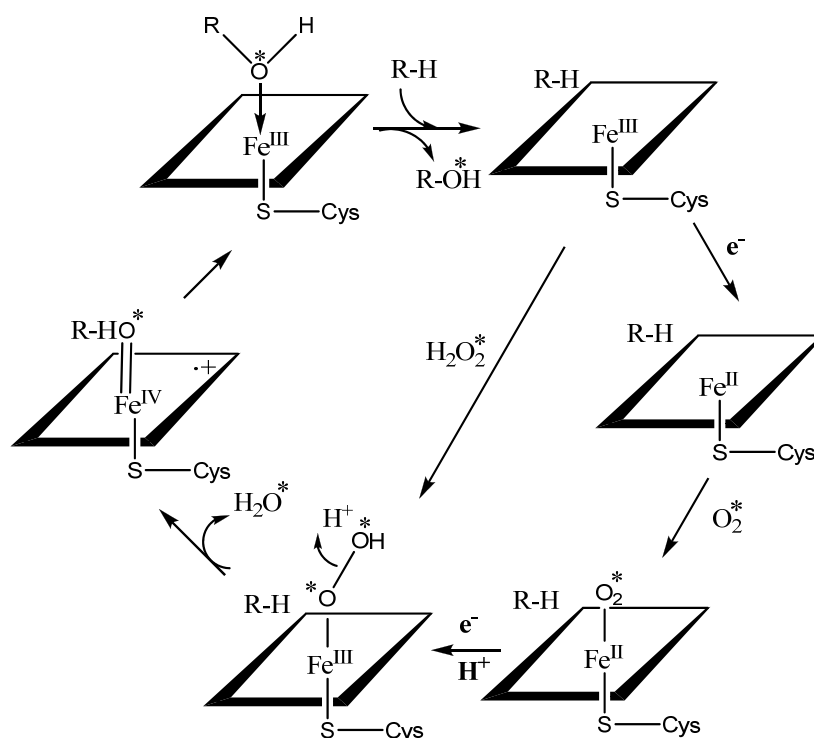
In the 1950s, Hayaishi first suggested activation and transfer of molecular oxygen by an iron-containing enzyme.³¹ This discovery changed the traditional view that the

oxygen in biological molecules is from water exclusively. A subsequent study revealed the mechanisms of molecular oxygen activation and transfer catalyzed by CYP450s and novel iron redox chemistry.

The major reactions catalyzed by CYP450 are alkane hydroxylation.³² For example, the most common reaction is that an organic substrate is oxidized by insertion of oxygen.



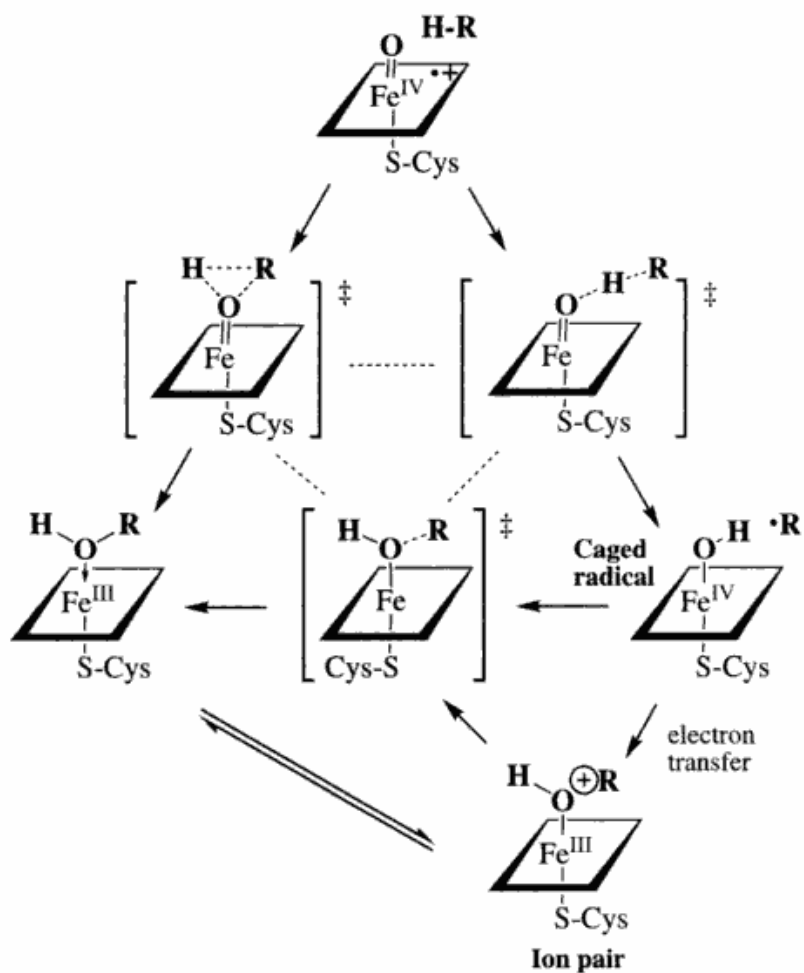
The mechanism is shown as Scheme 2.5:



Scheme 2.5 Consensus catalytic cycle for oxygen activation and transfer by cytochrome P450²⁸

- 1) Substrate binds to enzyme to form an enzyme-substrate adduct.

- 2) One electron can be transferred from NAD(P)H via electron transfer chain, reducing the ferric iron to the ferrous iron.
- 3) Molecular oxygen binds to ferrous heme to form P450-dioxygen complex.
- 4) Another one-electron reduction and protonation occurs to form Fe(III)-hydroperoxy complex.
- 5) The above complex is protonated and one water molecule is released to form iron-oxo intermediate.
- 6) ROH is released as final product.



Scheme 2.6 Possible pathway for oxygen-atom transfer from the active ferryl species to form the alcohol²⁸

CYP450 can oxidize saturated hydrocarbons, even as stable as cyclohexane. Not like reactions performed by chromates and permanganate, the hydroxylations catalyzed by iron-containing enzymes occur selectively under mild conditions. This property attracted many researchers' attention. The possible mechanism is shown in the above scheme 2.6. The caged radical and ion pair may be formed during rearrangement.

Much of the interest in CYP450 research has focused on human CYP450s. CYP450s are the major enzymes that metabolize drugs, thus, it is extremely important to study human CYP450s in the pharmaceutical industry. Since the first human P450 was identified and purified in the late 1970s, all 57 human P450 genes have been identified.^{28,33-35} CYP450s have been found in many tissues, such as liver, lung, kidney and brain. Most of them exist in the endoplasmic reticulum (microsomal CYP450s); only 6 out of 57 are located in mitochondria.²⁸

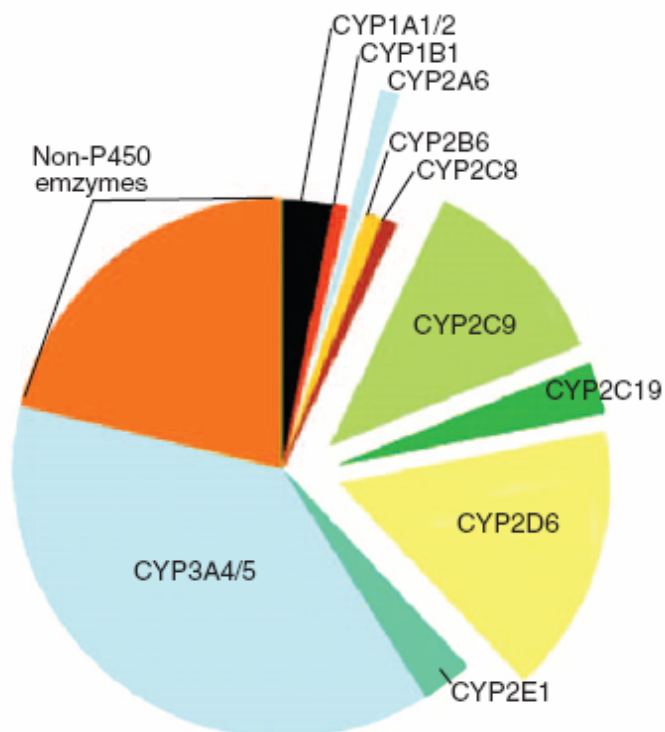


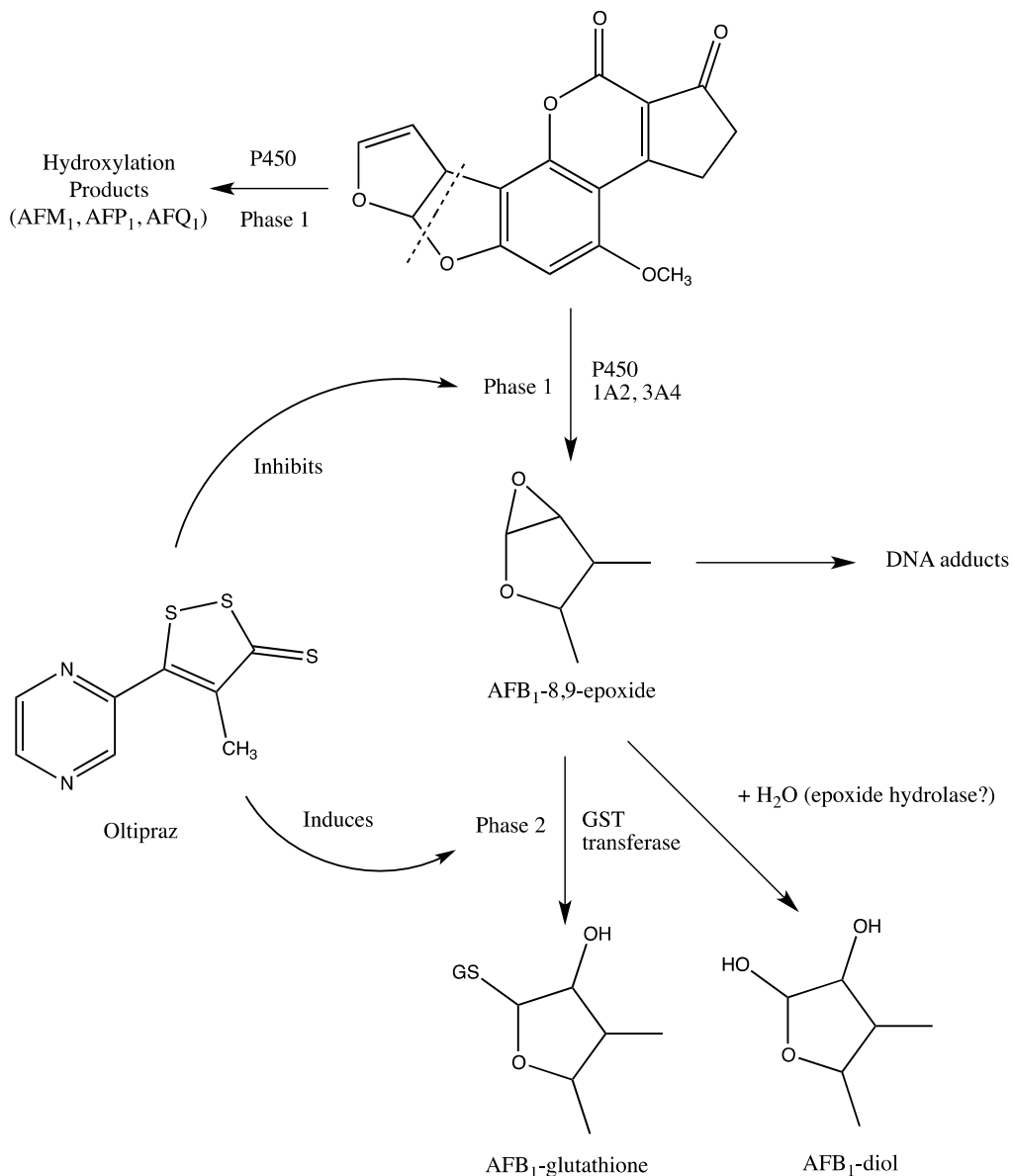
Figure 2.3 Contribution of major human P450s to the Phase I metabolism of all drugs currently marketed⁴²

The study of individual human CYP450s demonstrated that three major CYP450s (3A4, 2D6, 2C9) account for ~75 % of drug metabolism, and 90~95 % of all drug metabolism can be performed by 6~7 CYP450s (Figure 2.3).³⁶ CYP450s also metabolize chemical carcinogens, but this metabolism usually involves CYP 1A1, 1B1, 2A6, and 2E1 instead of 2C19 and 2D6.³⁷

2.3 Chemoprevention compounds against AFB1

Several chemoprevention compounds have been developed against AFB1-induced cytotoxicity and carcinogenic activity, such as oltipraz and chlorophyllins.³⁸⁻⁴¹ Oltipraz

can inhibit the phase one CYP450 enzyme and meanwhile induce phase two glutathione S-transferases (GSTs), which permit the formation of AFB₁-glutathione conjugates, thus, preventing the formation of AFB₁-DNA complex (Scheme 2.7). But the drawbacks of oltipraz are that it may cause acute gastrointestinal toxicity and induce estrogen responsive genes.



Scheme 2.7 Effect of oltipraz on the metabolism of aflatoxin B₁³⁹

Chlorophyllin is another compound, which is in clinic trial. It diminishes the bioactivity of AFB1 by forming a complex with it, but its low complex constant and high water solubility lead to a high dose requirement and low effectiveness. Moreover, more mechanistic studies are required for chlorophyllin.

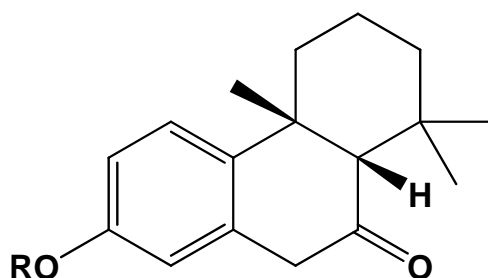
Most chemoprevention compounds focus on phase two enzymes to induce the formation of the AFB1-glutathione complex, while Chlorophyllin can form a complex with AFB1 by itself. Although there are several effective P450 inhibitors, there are few reported in the chemoprevention against AFB1. These findings suggest that new chemoprevention compounds against AFB1 induced cell cytotoxicity are needed. Therefore, our goal was to search for new chemoprevention compounds that may inhibit the phase one CYP450 enzyme to block the formation of AFB1 epoxide.

Chapter 3

Chemoprotective Actions of Hydroxy-Cis-Terpenone (HCT) Against Aflatoxin

3.1 Actions of HCT on liver cell viability

The cis-terpenone HCT and its analogs (Scheme 3.1) have been designed and synthesized in Dr. Zhou's lab. As mentioned above, Dr. Zhou predicted that the cis-terpenones would be hydroxylated and oxidized in liver cells, and the predicted metabolite that resembles resveratrol, would inhibit cytochrome P450 activity. If this hypothesis is correct, we would expect the metabolites to block the conversion of AFB1 to AFB1 exo-8,9-epoxide and therefore, protect cells. As a first step in testing this hypothesis, we examined the effects of cis-terpenones on the viability of HepG2 cells exposed to AFB1.



R= Me; H; Ac

Scheme 3.1 Structure of cis-terpenone analogs

Methods:

All chemicals were purchased from Fisher Scientific (Pittsburgh, PA) or Sigma-Aldrich (Milwaukee, WI) and used without further purification. NMR spectra of the synthesized compounds were obtained by Varian NMR spectrometers. Electrospray ionization mass spectroscopy (ESI-MS) analysis was carried out with Q-TOF2 from Micromass (Manchester, U.K.).

2-(3-Methoxybenzyl)-2-(2,6-dimethylhepta-1,5-dienyl)-1,3-dithiane (5). To a solution of thiol-protected citral as a 1:1 cis/trans mixture (1.10 g, 4.54 mmol) in dry THF (20 mL) at -40 °C (acetonitrile/dry ice bath) was slowly added a solution of 1.05 equiv of n-BuLi (1.6 M in hexanes, 2.84 mL) under N₂. The resulting reaction solution was stirred at -40 °C for 1 h, and then a solution of 3-methoxybenzyl chloride (650 mg, 4.16 mmol) in dry THF (10 mL) was added. The reaction mixture was maintained at -40 °C for 8 h and then slowly warmed to room temperature over 16 h under N₂. The reaction solution was quenched with brine (100 mL) and extracted with ether (100 mL X 2). The organic layers were collected, dried with MgSO₄, and concentrated. A flash column separation (0-2% EtOAc in hexanes) afforded the desired product as a cis/trans diastereoisomeric mixture (0.60 g) in 40% yield. Further separation of the isomers was not carried out because the subsequent cyclization step afforded diastereoisomerically pure cis compounds. ¹H NMR (CDCl₃, 300 MHz) for the cis/trans diastereoisomeric mixture: δ 7.23-7.14 (m, 1H), 6.95-6.72 (m, 3H), 5.40 (s, 1H), 5.19-5.05 (m, 1H), 3.83-3.76 (m, 3H), 3.37-3.25 (m, 2H), 3.00-2.74 (m, 4H), 2.54-2.44 (m, 1H), 2.17-1.90 (m, 5H), 1.84-1.52 (m, 9H). ¹³C NMR

(CDCl₃, 75 MHz) observed: δ 159.1, 143.2, 142.5, 137.8, 137.5, 132.0, 128.8, 128.7, 127.9, 127.4, 124.5, 124.3, 123.7, 117.0, 116.9, 112.5, 112.4, 55.3, 54.4, 47.0, 46.8, 41.8, 32.8, 28.2, 28.0, 26.9, 26.4, 26.0, 25.6, 24.7, 18.0, 17.9, 17.3. ESI-MS calcd for C₂₁H₃₁OS₂ (M - H⁺), 361.17; found, 361.07.

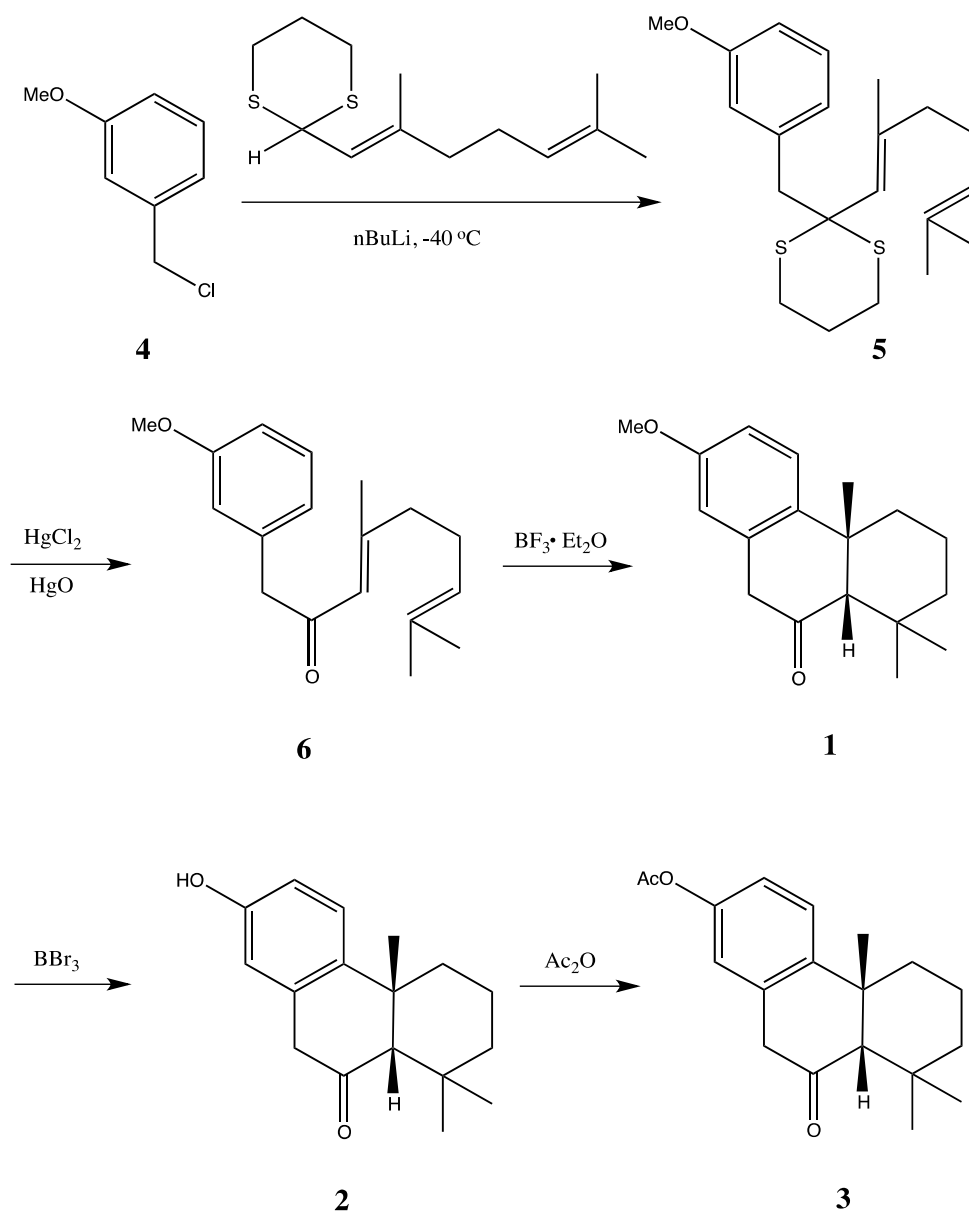
1-(3-Methoxyphenyl)-4,8-dimethylnona-3,7-dienyl-2-one (6). To a solution of 5 (300 mg, 0.83 mmol) in MeOH/H₂O (9:1, 25 mL) was added 1.1 equiv of HgO and HgCl₂. The resulting reaction solution was stirred at room temperature for 4 h. The reaction solution was diluted with CH₂Cl₂, and the precipitation was filtered through a 5 μ m Acrodisc filter. The solution was washed with brine, dried with MgSO₄, and concentrated. The desired product was purified by a flash column separation (0-10% EtOAc in hexanes) as a cis/trans diastereomeric mixture (160 mg) in 71% yield. ¹H NMR (CDCl₃, 300 MHz) for the cis/trans diastereomeric mixture: δ 7.24-7.14 (m, 1H), 6.84-6.74 (m, 2H), 6.09 (s, 1H), 5.05-4.98 (m, 1H), 3.79 (s, 3H), 3.74-3.67 (m, 2H), 2.18-2.09 (m, 7H), 1.17-1.56 (m, 6H). ¹³C NMR (CDCl₃, 75 MHz) observed: δ 198.1, 160.3, 160.0, 136.7, 132.7, 129.7, 129.5, 123.2, 123.1, 122.6, 122.1, 121.9, 119.7, 115.3, 115.2, 114.1, 113.0, 112.5, 64.1, 55.5, 55.3, 51.7, 46.7, 41.5, 34.2, 26.9, 26.3, 26.0, 25.9, 19.7, 17.9. ESI-MS calcd for C₁₈H₂₅O₂ (M + H⁺), 273.19; found, 273.07.

4b,5,6,7,8,8a-cis-Hexahydro-2-methoxy-4b,8,8-trimethylphenanthren-9(10H)-one (1). To a solution of 6 (130 mg, 0.48 mmol) in dry CH₃NO₂ (10 mL) at room temperature was added 10 equiv of BF₃•Et₂O, and the resulting reaction solution was stirred under N₂ for 2 h. The reaction solution was diluted with saturated NaHCO₃ (150

mL) and extracted with CH_2Cl_2 (150 mL X 3). The organic layers were collected, dried with MgSO_4 , and concentrated. The desired compound was purified by a flash column separation (0-5% EtOAc in hexanes) as a diastereoisomeric pure oil (50 mg) in 38% yield. ^1H NMR (CDCl_3 , 300 MHz): δ 7.23 (d, J) 8.7 Hz, 1H), 6.80 (dd, J1) 8.7 Hz, J2) 2.7 Hz, 1H), 6.61 (d, J) 2.7 Hz, 1H), 3.80 (s, 3H), 3.69 (d, J) 22.8 Hz, 1H), 3.48 (d, J) 22.8 Hz, 1H), 2.48 (d, J) 14.1 Hz, 1H), 2.10 (s, 1H), 1.54-1.46 (m, 2H), 1.34-1.23 (m, 3H), 1.05 (s, 3H), 0.95 (s, 3H), 0.34 (s, 3H). ^{13}C NMR (CDCl_3 , 75 MHz): δ 212.5, 158.2, 135.6, 134.0, 125.2, 113.9, 112.7, 66.7, 55.4, 44.4, 42.4, 38.3, 36.4, 34.4, 33.8, 32.4, 22.7, 19.0. ESI-MS calcd for $\text{C}_{18}\text{H}_{25}\text{O}_2$ ($\text{M} + \text{H}^+$), 273.19; found, 273.12.

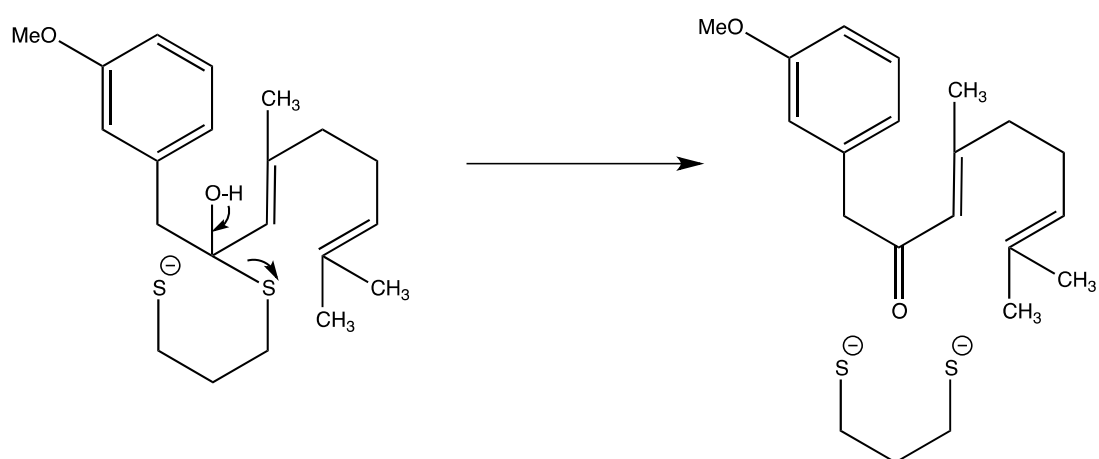
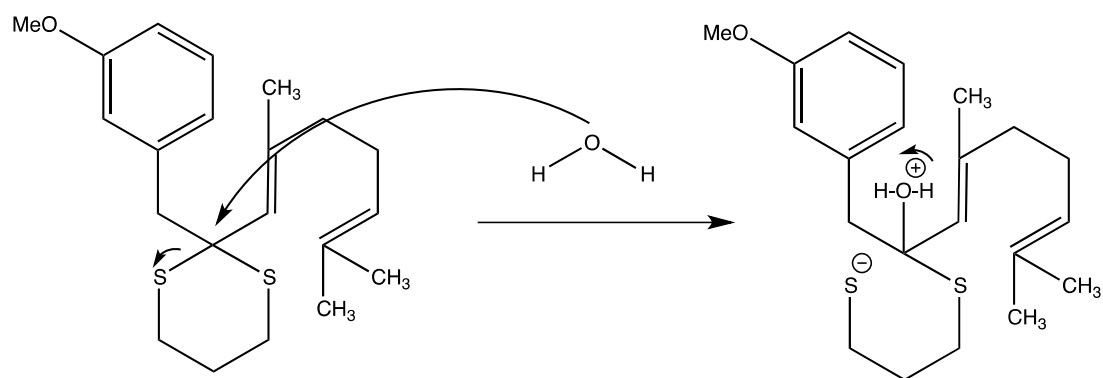
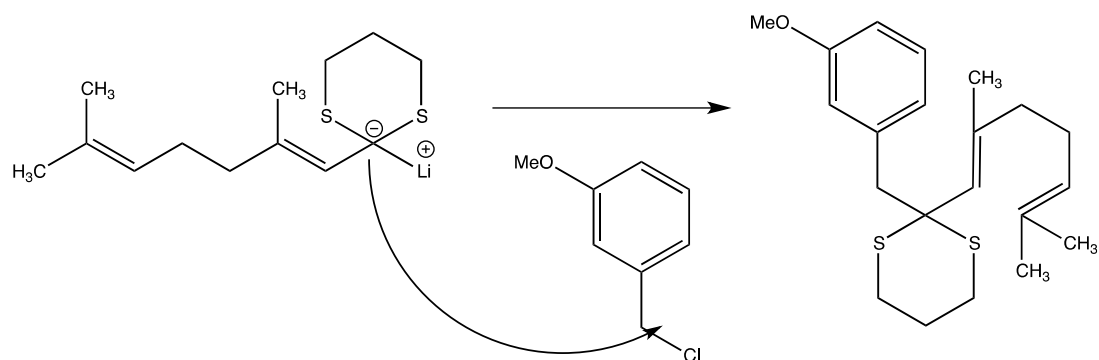
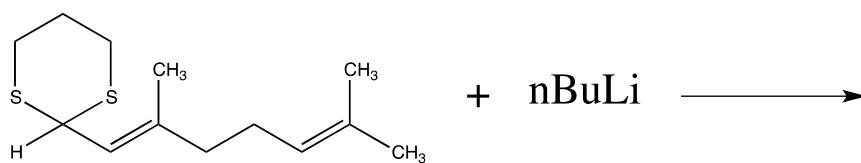
4b,5,6,7,8,8a-cis-Hexahydro-2-hydroxy-4b,8,8-trimethylphenanthren-9(10H)-one (2). To a solution of 1 (15 mg, 0.05 mmol) in CH_2Cl_2 (2.0 mL) under N_2 was added a solution of BBr_3 (1.0 M in heptane, 1.0 mL). The resulting solution was stirred at room temperature for 2 h. The reaction solution was quenched with brine (100 mL) and extracted with EtOAc (100 mL \times 2). The organic layers were collected, dried with MgSO_4 , and concentrated. A flash column separation (5-35% EtOAc in hexanes) afforded the desired product (8 mg) as an oil in 57% yield. ^1H NMR (CDCl_3 , 300 MHz): δ 7.18 (d, J) 8.7 Hz, 1H), 6.73 (dd, J1) 8.7 Hz, J2) 2.4 Hz, 1H), 6.57 (d, J) 2.4 Hz, 1H), 4.78 (bs, 1H), 3.67 (d, J) 22.8 Hz, 1H), 3.45 (d, J) 22.8 Hz, 1H), 2.48 (d, J) 12.3 Hz, 1H), 2.10 (s, 1H), 1.56-1.47 (m, 2H), 1.35-1.23 (m, 3H), 1.05 (s, 3H), 0.95 (s, 3H), 0.35 (s, 3H). ^{13}C NMR (CDCl_3 , 75 MHz): δ 212.6, 154.1, 135.9, 134.0, 125.4, 115.3, 114.2, 66.7, 44.2, 42.4, 38.3, 36.4, 34.4, 33.8, 32.4, 22.7, 19.0. ESI-MS calcd for $\text{C}_{17}\text{H}_{21}\text{O}_2$ ($\text{M} - \text{H}^+$), 257.15; found, 257.33.

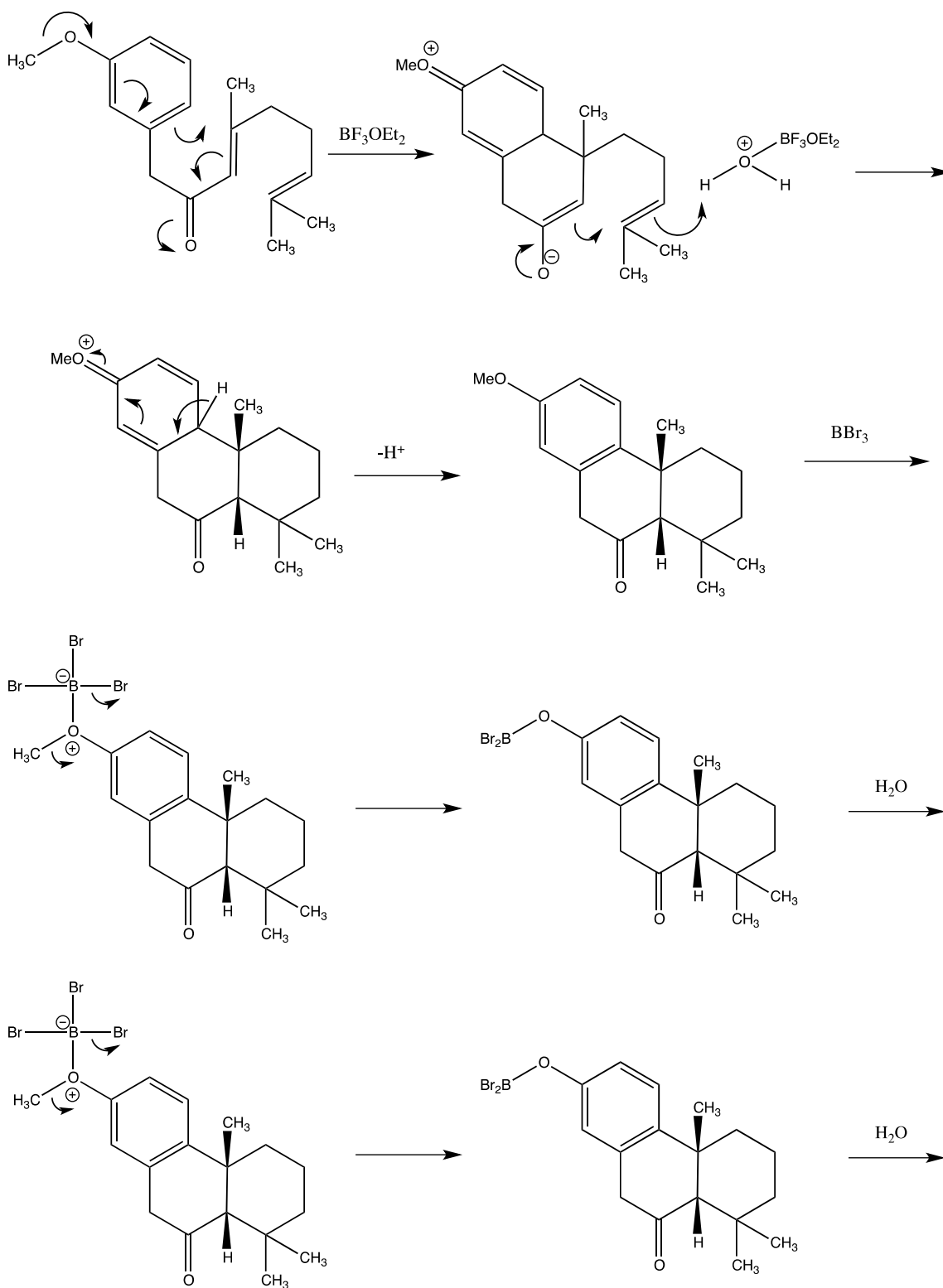
4b,5,6,7,8,8a-cis-Hexahydro-2-acetyloxy-4b,8,8-trimethylphenanthren-9(10H)-one (3). To a solution of 2 (5 mg, 0.02 mmol) in CH₃CN (2.0 mL) was added solutions of Ac₂O and Et₃N (1.0M, 1.0 mL each). The resulting solution was stirred at room temperature for 4 h. The reaction solution was extracted with Et₂O (50 mL X 2). The organic layers were collected, dried with MgSO₄, and concentrated. A flash column separation (5-20% EtOAc in hexanes) afforded the desired product (5 mg) as an oil in 84% yield. ¹H NMR (CDCl₃, 300 MHz): δ 7.33 (d, J) 8.7 Hz, 1H), 6.99 (dd, J1) 8.7 Hz, J2) 2.4 Hz, 1H), 6.83 (d, J) 2.4 Hz, 1H), 3.71 (d, J) 22.8 Hz, 1H), 3.50 (d, J) 22.8 Hz, 1H), 2.50 (d, J) 14.1 Hz, 1H), 2.29 (s, 3H), 2.12 (s, 1H), 1.56-1.48 (m, 2H), 1.37-1.23 (m, 3H), 1.07 (s, 3H), 0.95 (s, 3H), 0.33 (s, 3H). ¹³C NMR (CDCl₃, 75 MHz): δ 211.7, 169.7, 149.2, 139.3, 135.8, 125.2, 121.5, 120.3, 66.5, 44.2, 42.3, 38.7, 36.4, 34.5, 33.5, 32.3, 22.7, 21.4, 18.9. ESI-MS calcd for C₁₉H₂₃O₃ (M - H⁺), 299.16; found, 299.33.



Scheme 3.2 Synthesis of cis-Terpenones 1-3

Detailed mechanism is showed in Scheme 3.3.





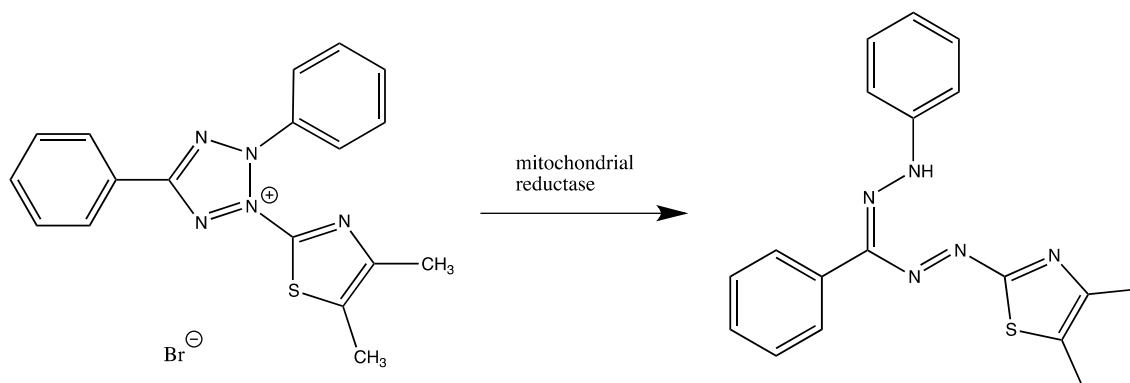
Scheme 3.3 Detailed synthesis mechanism of cis-Terpenes

Cells: Human HepG2 cells were obtained from ATCC (Manassas, VA) and maintained in 75 cm² flasks in the incubator at 37 °C with 5 % CO₂. The growth medium contained 90 % Minimum Essential Eagle medium (MEM) from Invitrogen (Carlsbad, CA) and 10 % heat-inactivated fetal bovine serum (FBS) plus 2 mM L-glutamine, 0.75 g/L sodium bicarbonate, 0.1 mM nonessential amino acids, 1.0 mM sodium pyruvate, 50 Unit/mL penicillin, and 50 µg/mL streptomycin.

MTT cell viability

MTT Assay

The MTT assay is a common colorimetric method used in the laboratory to test mitochondrial reductase activity of living cells. [MTT = (3-(4,5-Dimethylthiazol-2-yl)-2,5-diphenyltetrazolium bromide, a tetrazole)] Since mitochondrial reductase of dead cells cannot function properly, the MTT assay is also used to measure the viability of cells.



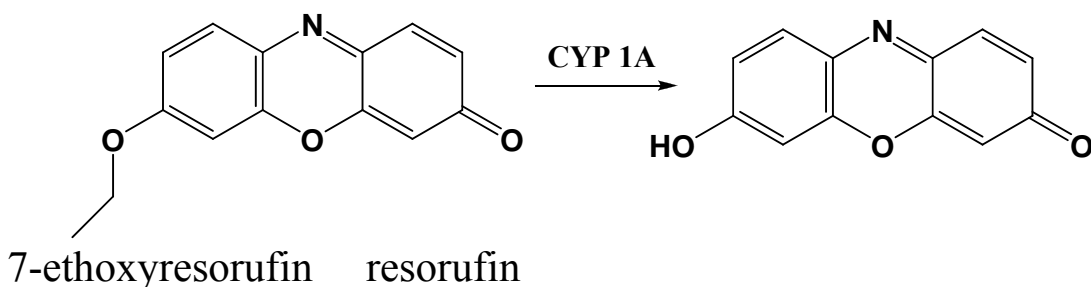
Scheme 3.4 MTT Reduction

The yellow color MTT (3-(4,5-Dimethylthiazol-2-yl)-2,5-diphenyltetrazolium bromide, a tetrazole) is reduced to the purple color formazan in the presence of mitochondrial reductase. By measuring the absorbance at different wavelength (570nm and 670nm), cell viability can be determined quantitatively.

The MTT (3-(4,5-Dimethylthiazol-2-yl)-2,5-diphenyltetrazolium bromide) solution was prepared at 5 mg/mL in PBS solution (pH 7.4), filtered, and stored at 4 °C. The MTT lysis buffer was prepared by dissolving 25 g of SDS in 100 mL of 50 % DMF in water, and the pH was adjusted to 4.7 with a solution of 2.5 % HCl in 80 % acetic acid. HepG2 cells were seeded in a 96-well cell cultured plate at 30,000 cells per well and maintained in 200 μ L of growth medium at 37° C for 4 hours prior to treatment with AFB1 and cis-terpenone compounds. Treatment included medium only, 2 μ M AFB1 only, 2 μ M AFB1 plus 10, 20, 40 μ M cis-terpenone and 40 μ M cis-terpenone only. The final DMSO concentration was kept at 0.15 %. After 72 hours incubation, 10 μ L stock MTT solution was added to each well and incubated overnight. After incubation, the medium solution was removed and 100 μ L MTT lysis buffer was added. After 10 hours, the absorbance of each well at 570 nm (background correction at 690 nm) was obtained with an iQuant plate reader (BioTek Instruments, VT).

Measurement of CYP 1A/B activity with the EROD assay:

EROD Assay



Scheme 3.57-ethoxyresorufin deethylation reaction

The ethoxyresorufin-O-deethylase (EROD) assay is widely used in bio labs to measure the amount of CYP 1A enzyme. 7-ethoxyresorufin acts as a substrate for CYP 1A and can undergo deethylation to form the product resorufin. The catalytic activity of this reaction indicates the present amount of CYP 1A. By measuring the fluorescence of resorufin, EROD assay provides a fast and direct method to detect CYP 1A enzyme. Dicumarol was added to the reaction to inhibit reductase activity.

HepG2 cells were seeded at 50,000 cells/well in a 96-well plate. After plating for 4 h, various treatments included DMSO only, TCDD only, TCDD plus cis-terpenes **1-3**, and cis-terpenes only. The final concentration of TCDD was 1 nM, and the concentrations of cis-terpenes **1-3** were 0.1, 1, 10, and 20 μ M. The final volume of each well was 200 μ L containing 0.1 % DMSO. After 24 h, the EROD assay was performed. Briefly, fresh medium (175 μ L per well) containing 2% serum, 8 μ M 7-

ethoxyresorufin, and 10 μ M dicumarol were added to each well and then incubated for 1 h. The resulting medium (150 μ L each) was transferred to a 96-well black plate, and ethanol (150 μ L/well) was added. The fluorescence intensity of each well between 580 and 600 nm was obtained by a Cary Eclipse fluorescence spectrometer (Varian Instruments, CA) with an exciting wavelength at 550 nm. The fluorescent intensity at 590 nm (λ_{max}) was used as the index for EROD activity, and statistical analyses (one-way ANOVA with Dunnett's test) were performed with GraphPad Prism software. All of the experiments were independently repeated at least three times. Also, the cell viability MTT assay was carried out in a manner similar to that described above.

Results and discussion:

As to confirm the stereochemistry of our cis-terpenone compounds, one of the compounds was performed 2D NOESY NMR spectrum.

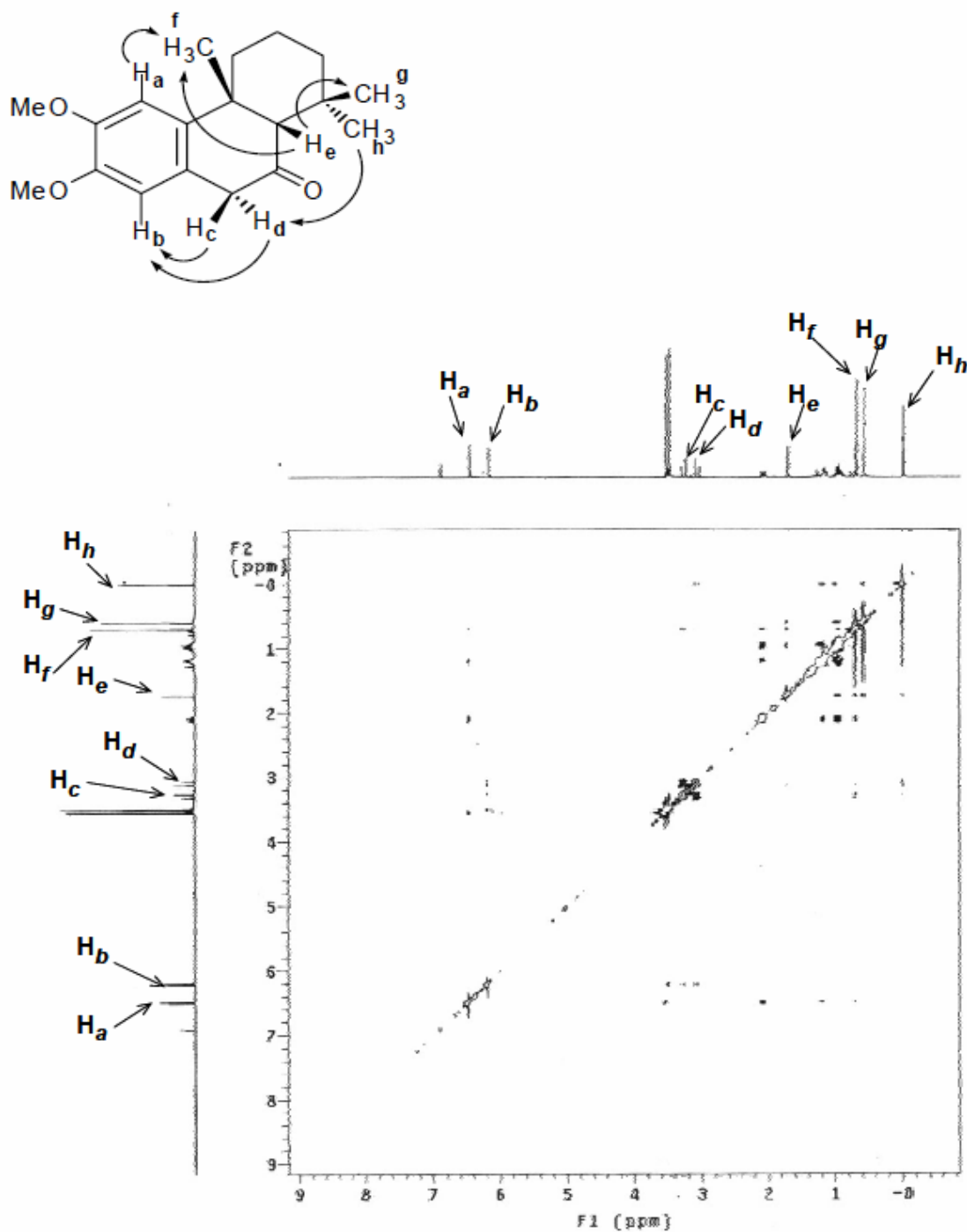


Figure 3.12 2D NOESY NMR Spectrum of cis-terpenone compound

Clearly, figure 3.2 shows no cytotoxicity when cells were treated with a high concentration (40 μ M) of cis-terpenones for 72 hours.

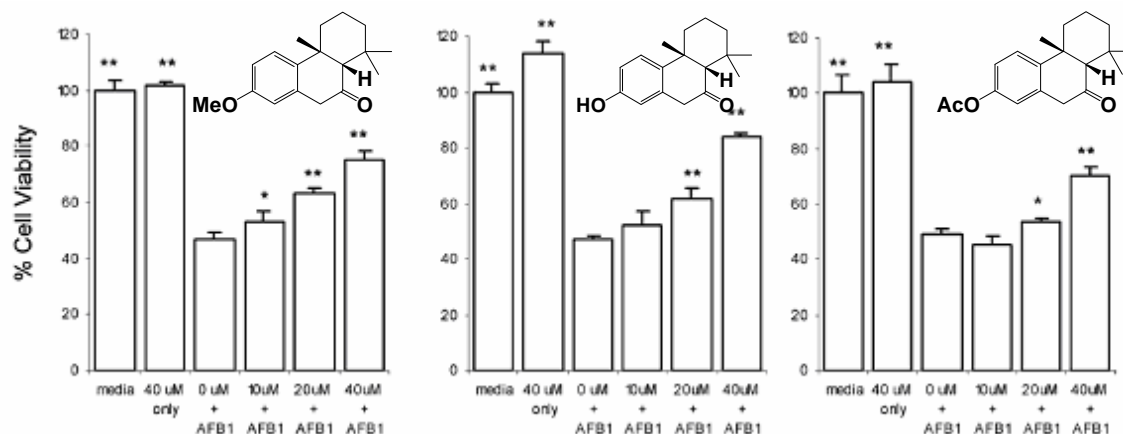


Figure 3.2 Chemo-protection with cis-terpenones against AFB1-induced cytotoxicity. HepG2 cells were co-treated with AFB1 (2 μ M) and cis-terpenones 1-3 at various concentrations (10-40 μ M) and incubated for 72 h. The percentage of viable cells was based on cells treated with medium only. Each bar represents the mean \pm SD of four replicates. The data are representative of three independent experiments. * $P < 0.05$ and ** $P < 0.001$ compared to treatment with AFB1 by one way ANOVA and Dunnett's test.

Second, we treated cells with AFB1 at 2 μ M and co-treated with AFB1 and different cis-terpenones at various concentrations (10-40 μ M). From the above Figure, we can clearly see that 2 μ M AFB1 caused 50 % cell death. When cis-terpenones were combined with AFB1 in HepG2 cells, increasing cell viability was observed (up to 80 % at 40 μ M). This suggests that our cis-terpenone compounds may be potential chemoprevention compounds against AFB1.

3.2 Actions of Cis-Terpenones on Cytochrome P450 (CYP450)

In the previous AFB1 inhibition studies, we showed that cis-terpenones had promising chemoprevention effects on AFB1-induced cell cytotoxicity. Our next project was to reveal the mechanism of cis-terpenones inhibition of AFB1. Since the toxic AFB1 exo-8,9-epoxide metabolite is formed from AFB1 by cytochrome P450 (CYP450), we decided to investigate whether cis-terpenones block the activity of CYP450.

In order to examine the inhibition mechanism of our cis-terpenone compounds, we first investigated effects of the cis terpenones on induction of CYP1A/B activity in HepG2 cells. The family-1 of CYP450 is induced in many cells by carcinogens and other compounds, and is of great research interest due to its involvement in cancer development. CYP family-1 includes CYP 1A1, 1A2, and 1B1. Both CYP 1A1 and 1B1 are known to activate a large variety of chemical carcinogens that result in cell damage and initiation of tumor development.⁴²⁻⁴⁴ For example, both benzo[a]pyrene and aflatoxin B1 are converted by CYP 1A1 and 1B1 to reactive metabolites resulting in DNA damage.^{45,46} Since the actual CYP1A/B amount in HepG2 cells is undetectable, 2,3,7,8-tetrachlorodibenzo-p-dioxin (TCDD) was used to induce CYP1A/B activity.⁴⁷ Indeed, as described below, we found that cis-terpenone compounds at 10 μ M can inhibit TCDD-induced CYP1A/B activity by 50 % compared to control.

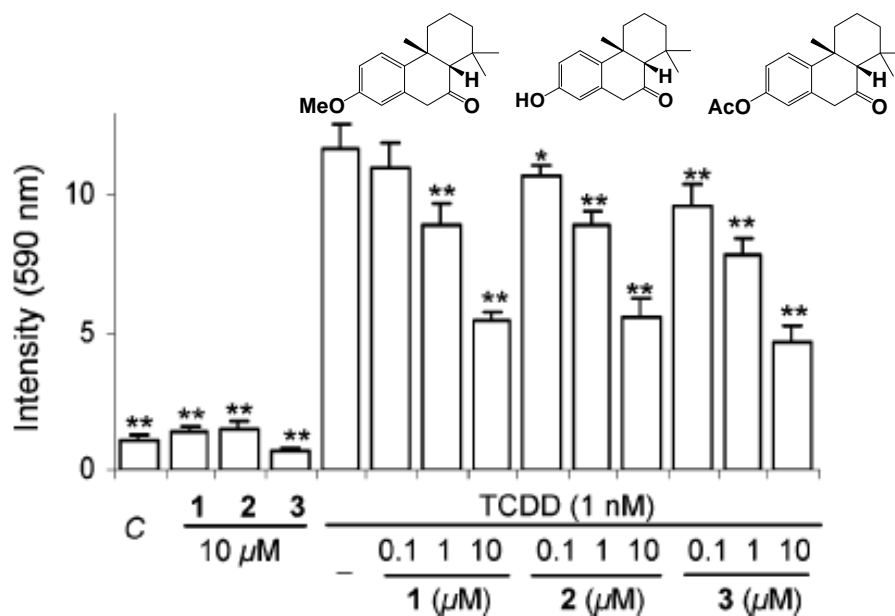


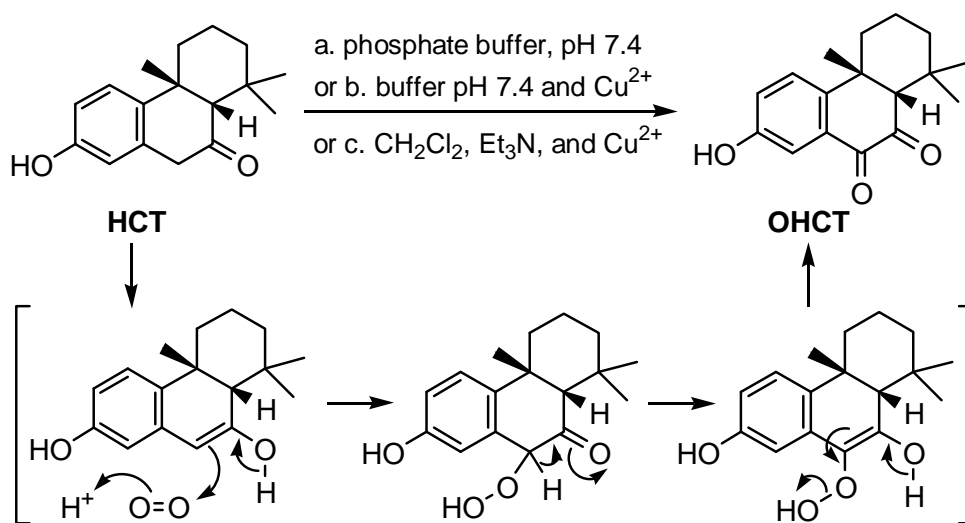
Figure 3.3 Inhibition of TCDD-induced P450 1A/B activity with *cis*-terpenes. HepG2 cells were co-treated with TCDD (1 nM) and *cis*-terpenes **1**, **2** or **3** and incubated for 24 h. The activity of P450 1A/B was determined with the EROD assay. Bars represent the mean \pm SD of EROD activity at 590 nm in 4 replicates. The data are representative of three independent experiments. C: Vehicle (0.1 % DMSO) only. * $P < 0.05$, ** $P < 0.001$ compared to TCDD only with one way ANOVA and Dunnett's test.

We found that *cis*-terpenes can effectively inhibit TCDD-induced P450 1A/B activity in HepG2 cells as shown in Figure 3.3. Without TCDD treatment, P450 1A/B activity is very low, whereas TCDD (1 nM) significantly induced P450 1A/B activity. When co-treated with *cis*-terpenes and TCDD, P450 1A/B enzymatic activity decreased with increasing concentrations of *cis*-terpenes. *Cis*-terpenes **1-3** at 10 μ M reduced the induced 1A/B activity by approximately 50%. In addition, no cytotoxicity in HepG2 cells under these conditions was observed. These results implied that *cis*-terpenes **1-3** could be used as chemopreventive agents that inhibit the activity of P450 1A/B and thereby protect cells against AFB1 induced cytotoxicity. The inhibitory effect

with cis-terpenones may be due to either the inhibition of enzyme activity or the suppression of the expression level of the enzyme. Therefore, further study of the inhibitory mechanism with cis-terpenones **1-3** was undertaken.

3.3 Liver Microsomes and P450 3A4 Studies with HCT

Dr. Zhou used HPLC to investigate effects of hydroxy-cis-terpenone on the activation and conversion of AFB1 by purified human CYP450 3A4 in the presence and absence of human liver microsomes, which have high CYP450 3A4 activity.^{33,34} Effects of both HCT and oxidized HCT (OHCT) were investigated because Dr. Zhou determined that HCT is converted to OHCT in aqueous media at pH 7.4, the normal pH of human plasma.



Scheme 3.6 OHCT as the Spontaneous Oxidation Product of HCT⁵⁰

Effects of cis-terpenones were compared with those of ketoconazole, a well known inhibitor of CYP450s, cholesterol as a structural analogue of HCT, and α -naphthoflavone, which is able to change the metabolite profile of AFB1 metabolism with P450 3A4 by enhancing the production of *exo*-AFB1-epoxide and reducing that of aflatoxin Q₁.⁴⁸

To assist with this study, I used the MTT assay to compare the cytotoxicity of ketoconazole, HCT and oxidized HCT on HepG2 cells. The cytotoxicity of benzopyrene on HepG2 cells was also tested by me.

Dr. Zhou found that 1 μ M ketoconazole inhibited the P450 3A4 activity in isolated human liver microsomes (Sigma) to the same extent as 40 μ M HCT and OHCT, that is the metabolite product of HCT (Fig. 3.4 and Fig. 3.5).⁵⁰ Although 20 μ M ketoconazole had the same effect as 40 μ M OHCT against cell cytotoxicity induced by 2 μ M AFB1 (Fig 3.6), this concentration of ketoconazole caused 20% cell death while HCT and OHCT exhibited no cytotoxicity, even at 60 μ M. This implied that HCT and OHCT were less toxic than ketoconazole when they were used to treat live cells, therefore, HCT and OHCT may be used as an alternative compound instead of ketoconazole.

In addition, cholesterol was included as the structural control in the study because cholesterol has a similar carbon skeleton as that of HCT. However, no inhibitory effect was observed with cholesterol up to 100 μ M, which indicated that the inhibitory effect of

HCT on the metabolic conversion of AFB1 was unique to the functional groups and stereochemistry of HCT.

The results of the above experiments implied that that both HCT and OHCT block the conversion of AFB1 to AFB1-epoxide by CYP450 3A4.

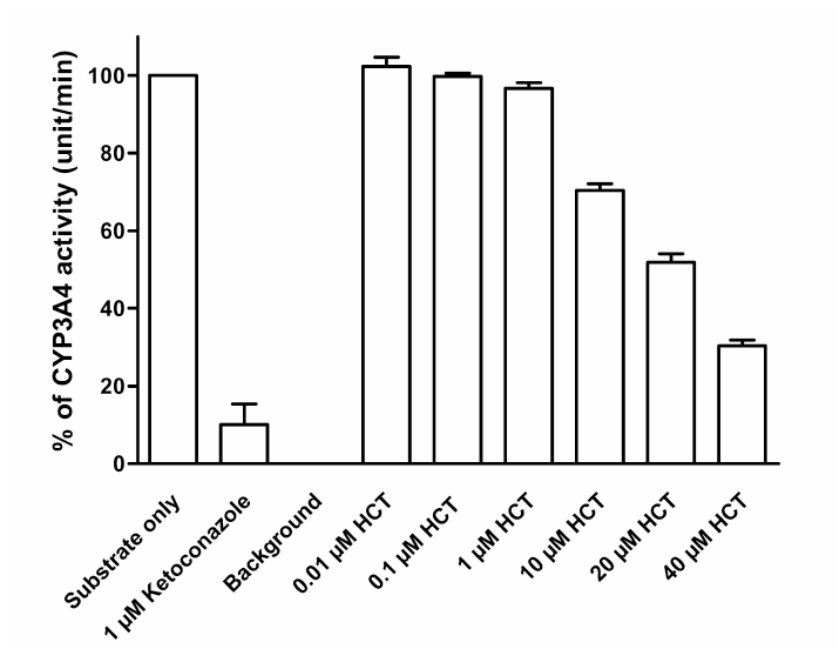


Fig 3.4 Inhibitory effects of HCT on the activity of purified P450 3A4⁵⁰

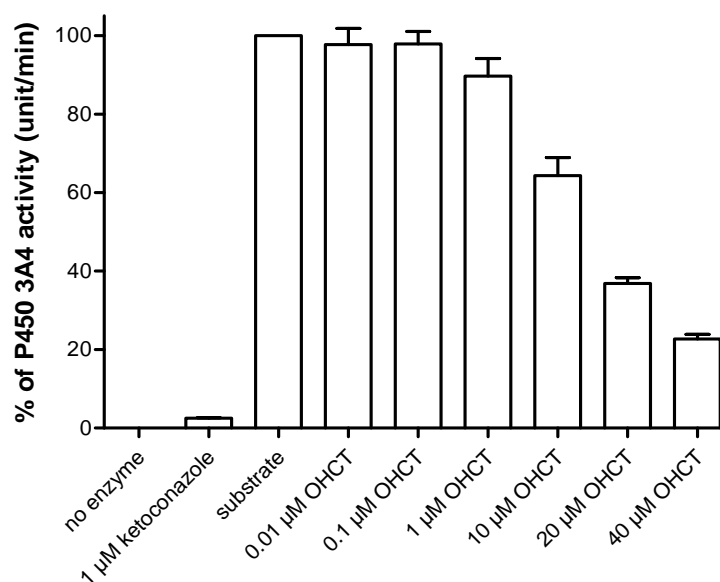


Fig 3.5 Inhibitory effects of OHCT on the activity of purified P450 3A4⁵⁰

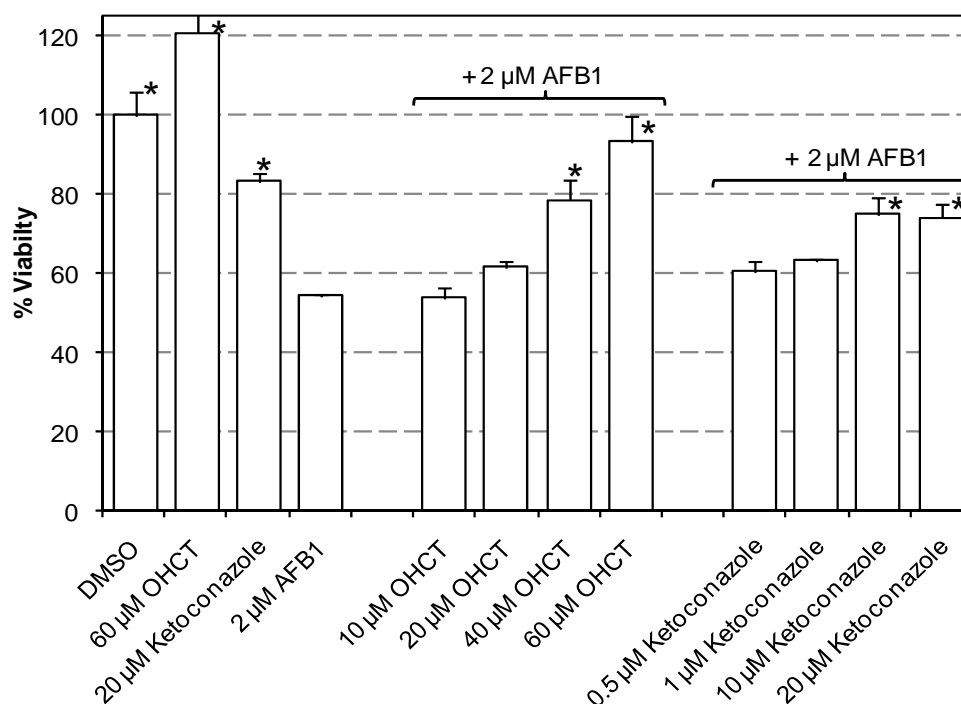


Fig 3.6 Chemo-protection with OHCT and ketoconazole against AFB1-induced cytotoxicity. HepG2 cells were co-treated with AFB1 (2 μ M) and OHCT and ketoconazole at various concentrations (10-60 μ M) and incubated for 72 h. The percentage of viable cells was based on cells treated with medium only. Each bar

represents the mean \pm SD of four replicates. The data are representative of three independent experiments. *P < 0.05 and **P < 0.001 compared to treatment with AFB1 by one way ANOVA and Dunnett's test.

Chapter 4

Actions of HCT on AFB1 Accumulation in HepG2 Cells

In the previous chapters, we demonstrated that novel *cis*-terpenones synthesized in our laboratory protect HepG2 cells against AFB1-induced cell death (up to 80 % at 40 μ M) for 72 hours.⁴⁹ Additionally, based on our CYP450 enzymes studies, we observed that these molecules reduce Phase I activation of AFB1 by CYP450 enzymes.⁵⁰ In order to further investigate the inhibitory mechanism of *cis*-terpenones, the following study was designed to determine whether *cis*-terpenones influence the uptake of AFB1 into HepG2 cells and secondarily to determine whether specific transporter proteins influence AFB1 accumulation in these cells.

4.1 Cellular Uptake and Efflux of AFB1

AFB1 is taken up by liver cells and metabolized to AFB1 epoxide-glutathione conjugates⁵¹⁻⁵⁵ which are excreted from cells by the multi-drug resistant protein-1 (MRP1),⁵³ an important efflux transporter in many cells.⁵⁶ MRP1 also transports unmodified AFB1, but the transport rate is low compared to that of conjugated AFB1 metabolites.⁵³ Chi and Devlin observed saturable uptake of AFB1 by rat hepatocytes,⁵⁵ but Müller and Petzinger reported that uptake of radiolabeled AFB1 in rat hepatocytes occurs primarily by non-ionic diffusion through the lipid membrane and is not saturated

by unlabeled AFB1.⁵³ No transport mechanism for AFB1 has been identified in human cells except for MRP1.

Methods:

Reagents: ³H-labeled AFB1 ([³H]-AFB1, 29.2 Ci/mole) was obtained from Moravek Biochemicals (Brea, CA). ³H-labeled estrone sulfate ([³H]-ES, 53-55 Ci/mole) was obtained from Perkin-Elmer. Unless specifically indicated, all other chemicals were purchased from Fisher Scientific (Pittsburg, PA) or Sigma-Aldrich (Saint Louis, MO) and used without further purification. Hydroxy- *cis*-terpenone (HCT) was synthesized as previously reported.¹³ Stock solutions of unlabeled AFB1 and HCT, carbamyl cyanide 4-(trifluoromethoxy) phenylhydrazone (FCCP), and omeprazole were prepared in dimethyl sulfoxide (DMSO) and stored at -20 °C. Estrone-3-sulfate potassium salt was dissolved in DMSO, and stock solutions of 17-β-estradiol, corticosterone, nigericin sodium salt, and verapamil were prepared fresh in ethanol prior to dilution in uptake buffer (described below). Stocks of 17-β-estradiol glucuronide were prepared in 0.1 M KOH and stored at -20 °C. Probenecid was dissolved in uptake buffer, and the pH was adjusted to 7.4 with KOH prior to use. Stocks of para-amino-hippuric acid, desipramine, glutathione (GSH), glutathione ester (GSHE), N-ethyl maleimide (NEM), and dithiothreitol (DTT) were prepared in deionized water and stored at -20 °C. Final concentrations of DMSO or ethanol in cell assays were kept below 0.2%.

Cells: Human HepG2 cells were obtained from ATCC (Manassas, VA) and maintained in 75 cm² flasks in the incubator at 37 °C with 5 % CO₂. The growth medium contained 90 % Minimum Essential Eagle medium (MEM) from Invitrogen (Carlsbad, CA) and 10 % heat-inactivated fetal bovine serum (FBS) plus 2 mM L-glutamine, 0.75 g/L sodium bicarbonate, 0.1 mM nonessential amino acids, 1.0 mM sodium pyruvate, 50 Unit/mL penicillin, and 50 µg/mL streptomycin.

Chinese hamster ovarian cells (CHO cells) transfected with the human OATPB gene and wild type (WT) CHO cells were obtained from Dr. Bruno Stieger, University of Zürich, Switzerland. The CHO cells were maintained in DMEM 12320332 (Invitrogen) supplemented with 50 Unit/mL penicillin and 50 µg/mL streptomycin, 10 % heat-inactivated FBS, and 50 mg/L proline. The medium for the cells transfected with OATPB also contained geneticin G-418 (500 mg/L) to select for the neomycin resistance of the transfected cells.

Transport assay:

Cells were seeded in a 24 well plate at 10⁶ cells / well and maintained in 1 mL of growth medium at 37° C in the incubator for 16 h prior to the transport assay. For the assay, the plate was removed from the incubator and kept at room temperature for 20 min to equilibrate. Cells were washed twice with 1 ml of sucrose/Hepes (SH) buffer, which contained 0.32 M sucrose and 10 mM Hepes adjusted to pH 7.4 with KOH. The final SH wash was removed at 1.5 min intervals, and cells were incubated for the times indicated

at room temperature in 0.8 ml of uptake buffer containing radiolabeled substrate 15 nM [^3H]-AFB1 (or where indicated [^3H]-estrone sulfate ([^3H]-ES), and inhibitors or competitive substrates or vehicle. For most assays the uptake buffer was that used by Finn et al for sodium-independent vesicular transport⁵⁷ (SH supplemented with 4 mM MgSO_4 and 4 mM KCl). In selected assays the transport buffer contained SH supplemented with 140 mM NaCl, 2 mM KCl, 1 mM CaCl_2 , 1 mM MgCl_2 , and 5 mM glucose. Transport was stopped by removing the uptake buffer and washing twice with SH. After the wash, cells were lysed for 5 min in 0.8 mL of 0.2 M NaOH containing 1 % sodium dodecyl sulfate. To measure cellular accumulation of radioactivity, a 200 μL aliquot of each cell lysate was added to 5 mL of Scinti-Safe Plus-50% (Fisher Scientific, Fair Lawn, New Jersey), and counted in the LS6000 IC scintillation counter (Beckman/Coulter). A 200 μL aliquot of uptake buffer also was counted to verify the total amount of radioactivity added to cells. For determination of background radioactivity, cells incubated for zero time after addition of [^3H]-labeled substrate in uptake buffer were included in each assay. Background radioactivity was subtracted from all measurements of cellular radioactivity.

Binding Assay:

Human liver microsomes were purchased from Sigma (S2442). Each assay tube contained 0.1 μg of microsomal protein and 15 nM [^3H]-AFB1 or 15 nM [^3H]-estrone sulfate ([^3H]-ES) and inhibitors or vehicle as indicated in a total volume of 200 μL of uptake buffer as described for the transport assay. All incubations were conducted at 29

°C for the times indicated. The reaction was terminated by addition of 1.5 ml cold SH buffer and rapid filtration through 0.2 μ m Supor 200 membranes (Pall/Gelman # 60300) in a Millipore sampling manifold. The reaction tubes were washed three times with 1.0 ml of SH buffer, which was transferred to the filter and rapidly filtered as above. Filters were transferred to 5 mL of Scinti-Safe Plus-50% (Fisher Scientific), and radioactivity was measured with a Beckman LS6000IC scintillation counter.

Data Analyses: Data were analyzed with Prism version 4.00 (GraphPad Software Inc., San Diego, CA). All assays were repeated at least three times independently. Percentage values were transformed to arcsin and compared with the appropriate control by an unpaired t test or by analysis of variance (ANOVA) with Dunnet's post hoc test.

4.2 Results and Discussion:

As seen in Figure 4.1, [3 H]-AFB1 accumulation reached a maximum by 30 min, and 40 μ M HCT inhibited [3 H]-AFB1 accumulation by approximately 50 % at every time point.

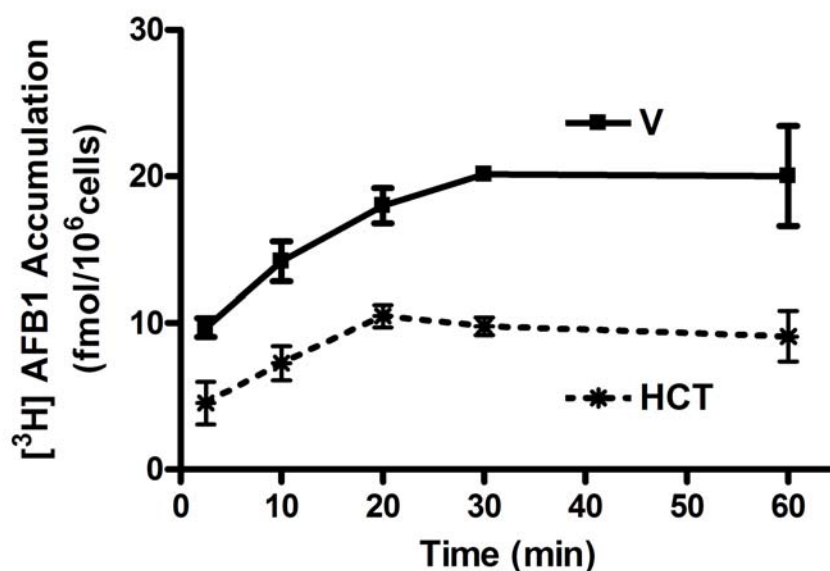


Figure 4.1 Time-dependent accumulation of [³H]-AFB1 by HepG2 cells. Cells were incubated with sodium-free uptake buffer containing 15 nM [³H]-AFB1 + vehicle (V) or [³H]-AFB1 + 40 μ M hydroxyl-*cis*-terpenone (HCT) for the times indicated. Cells were washed, lysed, and radioactivity was measured in 25% of the lysate. Background radioactivity measured at zero time was subtracted from each measurement. Points represent means \pm S.E. of at least 3 replicates obtained in separate experiments.

As shown in Figure 4.2, HCT inhibition of [³H]-AFB1 accumulation was concentration dependent, and the maximum was approximately 60 % at 60 μ M.

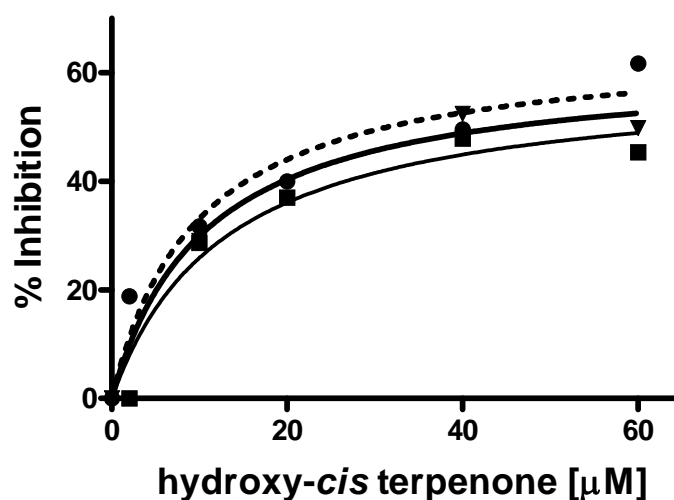


Figure 4.2 Concentration dependent inhibition of [3 H]-AFB1 accumulation with HCT. Accumulation in HepG2 cells was measured at 10 min as described in Figure 4.1. ($IC_{50} = 4\mu M$)

The co-treatment with unlabeled AFB1 decreased cellular accumulation of [3 H]-AFB1 as seen in Figure 4.3. These initial results suggested either saturation of a specific transport mechanism or saturation of AFB1 binding to internal cellular components, such as proteins. Inhibition of efflux would be expected to increase cellular accumulation of [3 H]-AFB1.

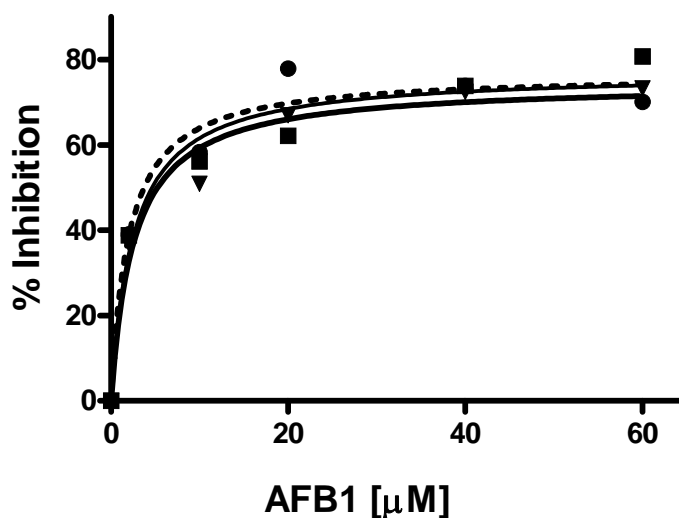


Figure 4.3 Concentration dependent inhibition of [3 H]-AFB1 accumulation with AFB1. Accumulation of [3 H]-AFB1 in HepG2 cells was measured at 10 min as described in Figure 4.1. ($IC_{50} = 2.4 \mu M$)

To investigate the ATP-dependence of AFB1 accumulation in HepG2 cells, the mitochondrial ATPase inhibitor sodium azide, which blocks activity of MRP1 and many other ATP-dependent transporters, was added to cells with or without HCT. No effect on accumulation of [3 H]-AFB1 was observed in the presence of sodium azide in sodium-free and glucose-free buffer (Figure 4.4). Furthermore, no effects were observed when the experiment was repeated with a buffer containing sodium and glucose or with the ATPase inhibitor sodium orthovanadate (Na_3VO_4) at 1 mM (data not shown). These findings support the idea that HCT modulates an accumulation mechanism that is not ATP-dependent; however, others have reported that sub-lethal concentrations of NaN_3 do not completely block the high ATPase activity in HepG2 cells.⁵⁸ As indicated below, other methods were then used to determine whether specific transporters affect the accumulation of AFB1 in HepG2 cells.

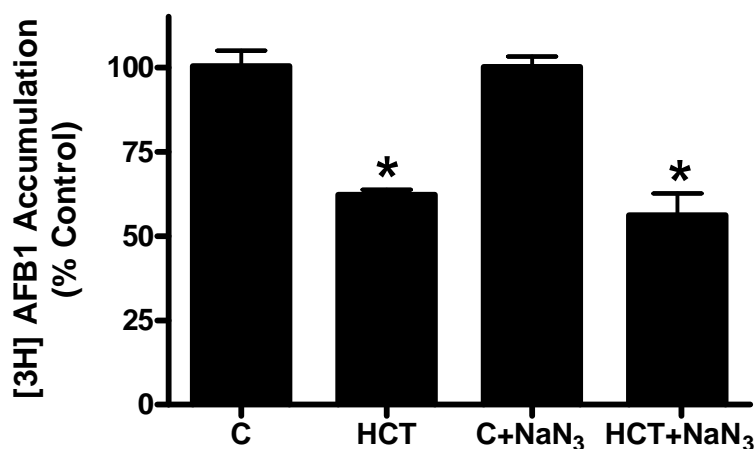


Figure 4.4 Effects of 3 mM sodium azide (NaN₃) on [³H]-AFB1 accumulation. Accumulation of [³H]-AFB1 was measured at 10 min in HepG2 cells treated with vehicle (V) or hydroxyl-*cis*-terpenone at 40 μ M (HCT). Bars represent mean \pm S.E. of at least 3 replicates. * $P < 0.01$.

To investigate uptake mechanisms for AFB1, buffer substitutions and several inhibitors or competitive substrates of organic cation transporters (OCT), organic anion transporters (OAT/OATP), and multi-drug-resistant efflux transporters were screened, because many of these transporters are expressed in Hep G2 cells^{58–69} and transport neutral lipophilic molecules, such as AFB1. Concentrations were determined either by limits of solubility or the maximal range of concentration used by previous investigators to inhibit transport activity. Initial results of this screen are shown in Figure 4.5, and a follow-up of these experiments is shown in Fig. 4.6.

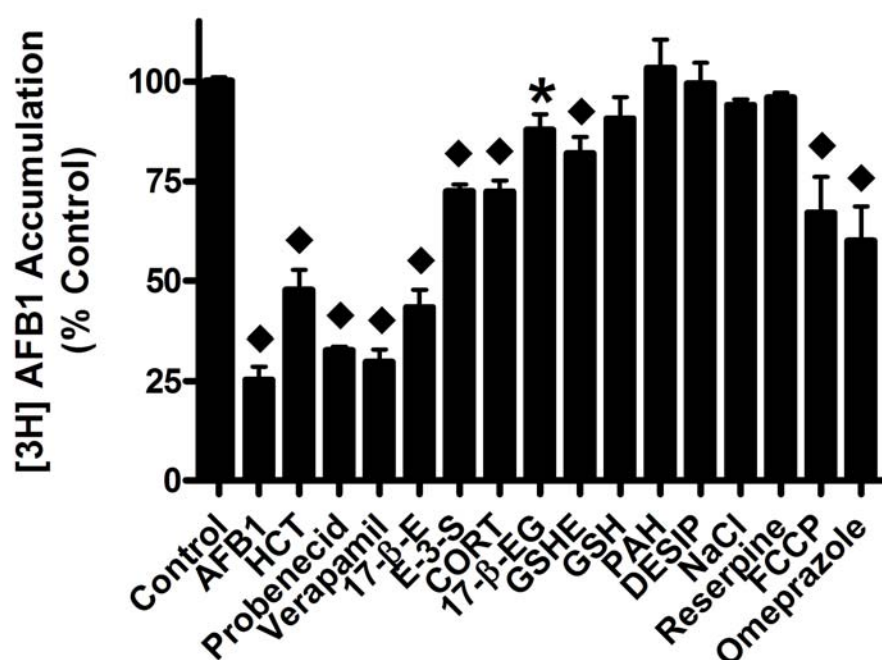


Figure 4.5 Effects of maximal concentrations of inhibitors and substrates on [³H]-AFB1 accumulation in HepG2 cells. Accumulation of [³H]-AFB1 in HepG2 cells was measured at 10 min as described in Figure 4.1. Bars represent the mean \pm S.E. of 3-4 replicates. * $P < 0.05$; ♦ $P < 0.01$ compared to the appropriate vehicle for each treatment. Concentrations: Control, vehicles only; 60 μ M AFB1, 60 μ M hydroxy cis-terpenone (HCT), 500 μ M probenecid, 500 μ M verapamil, 200 μ M 17- β -estradiol (17- β -E), 200 μ M 17- β -estradiol glucuronide (17- β -EG), 5 mM glutathione ethyl ester (GSHE), 5 mM glutathione (GSH), 80 μ M estrone-3-sulfate (E-3-S), 50 μ M corticosterone (CORT), 1 mM para-amino-hippuric acid (PAH), 50 μ M desipramine (DESIP), 4 mM NaCl, 1 μ M reserpine, 5 μ M carbamyl cyanide 4-(trifluoromethoxy) phenylhydrazine (FCCP), 100 μ M omeprazole.

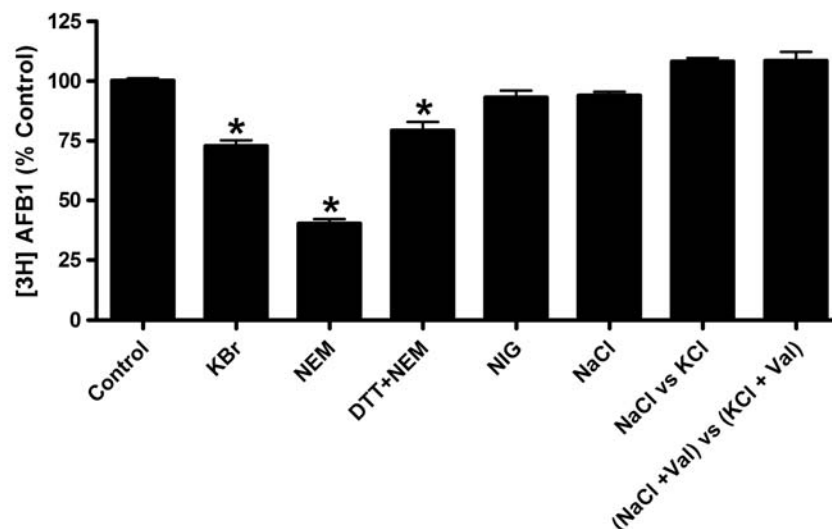


Figure 4.6 Effects of ions and N-ethylmaleimide on $[^3\text{H}]$ -AFB1 accumulation in HepG2 cells. Accumulation of $[^3\text{H}]$ -AFB1 in HepG2 cells was measured at 10 min as described in Figure 4.1. Bars represent the mean \pm S.E. of 3-4 replicates. * $P < 0.05$; $\diamond P < 0.01$ compared to the appropriate vehicle for each treatment. Control – Average of vehicles in each experiment. Concentrations: 4 mM KBr substituted for KCl in the uptake buffer, 500 μM N-ethylmaleimide (NEM), 500 μM dithiothreitol (DTT), 1 μM nigericin (NIG), and 10 μM Valinomycin (Val) -all in uptake buffer.

Because greater than 50 % inhibition of $[^3\text{H}]$ -AFB1 accumulation was observed with verapamil, probenecid, and 17- β -estradiol, additional assays were performed to determine the concentration-dependence of the inhibition (Figure 4.7, 4.8, and 4.9).

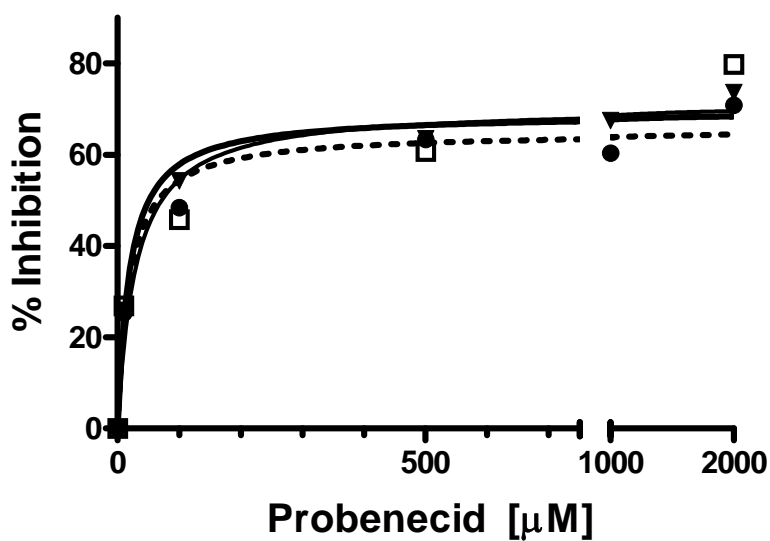


Figure 4.7 Inhibition of [3 H]-AFB1 accumulation with probenecid in HepG2 cells. Accumulation of [3 H]-AFB1 in HepG2 cells was measured at 10 min as described in Figure 4.1 ($IC_{50} = 30 \mu M$)

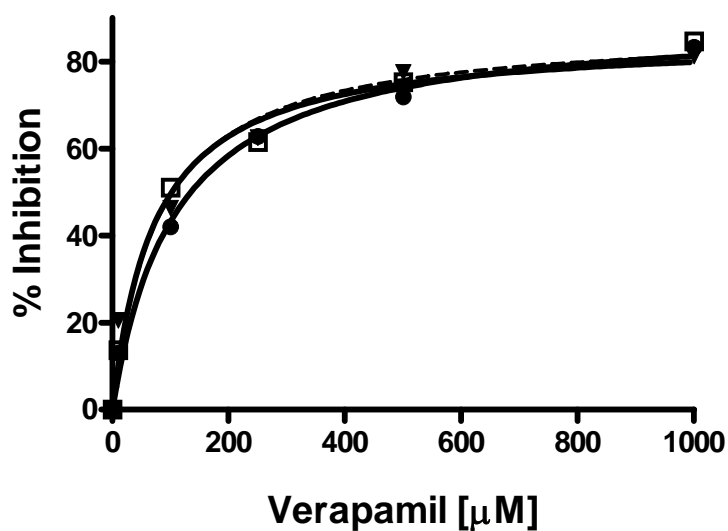


Figure 4.8 Inhibition of [3 H]-AFB1 accumulation with verapamil in HepG2 cells. Accumulation of [3 H]-AFB1 in HepG2 cells was measured at 10 min as described in Figure 4.1 ($IC_{50} = 100 \mu M$)

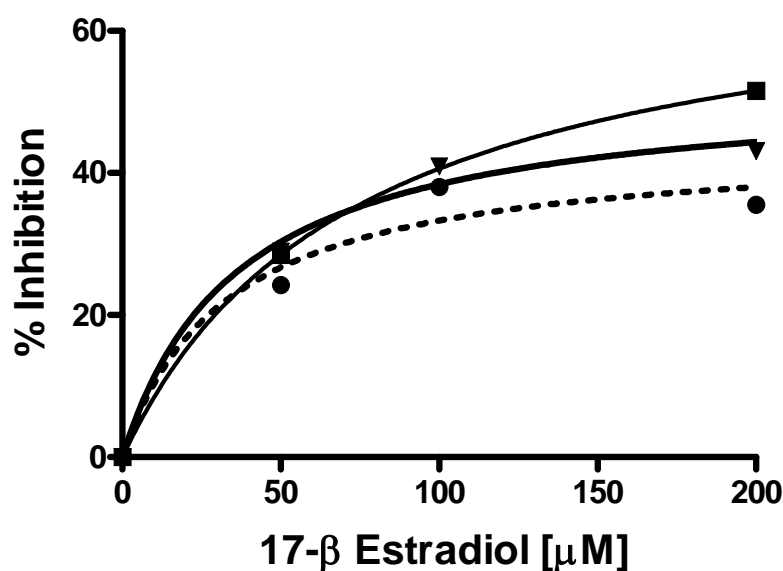


Figure 4.9 Inhibition of [^3H]-AFB1 accumulation with 17- β -Estradiol in HepG2 cells. Accumulation of [^3H]-AFB1 in HepG2 cells was measured at 10 min as described in Figure 4.1. ($\text{IC}_{50} = 30\mu\text{M}$).

Accumulation assays initially were performed with the sodium-free uptake buffer, and substitution of 4 mM NaCl for 4 mM KCl did not affect [^3H]-AFB1 transport (Fig. 4.5). Substitution of a transport buffer containing 140 mM NaCl also had no apparent effect on accumulation of [^3H]-AFB1 (data not shown). Reserpine, which inhibits both vesicular transporters and most MDR efflux transporters,⁶⁸ had no effect on accumulation of [^3H]-AFB1 (Fig. 4.5). These results suggested AFB1 accumulation in Hep G2 cells is not dependent on sodium, vesicular transporters, or most transporters in the MDR transporter family, at least under the conditions of the assay.

Verapamil inhibits organic cation uptake transporters OCT 1, 2 and 3 and the multi-drug resistant efflux transporter MDR1 (also known as p-glycoprotein). Although HepG2 cells express MDR1,^{62,65-68} inhibition of this efflux transporter would be expected

to increase accumulation of substrates. Failure of verapamil to increase accumulation of [3 H]-AFB1 was consistent with absence of reserpine effects on accumulation (Fig. 4.5) suggesting MDR1 was not involved in AFB1 transport. Inhibition of [3 H]-AFB1 by verapamil (Fig. 4.5 and 4.8) suggested OCTs may be involved in AFB1 transport, but the OCT inhibitor desipramine showed no effect on [3 H]-AFB1 accumulation (Figure 4.5). These findings suggested verapamil blocked accumulation of [3 H]-AFB1 by another mechanism, and we then investigated whether verapamil inhibits binding of [3 H]-AFB1 to intracellular proteins.

As described in Chapter 3, AFB1 is activated by CYPs in liver microsomes. Binding of AFB1 to microsomal enzymes could account for saturable accumulation in cells. We tested the hypothesis that unlabeled AFB1 and other lipophilic molecules, such as HCT and verapamil, inhibit binding of [3 H]-AFB1 to liver microsomal proteins. As illustrated in Figure 4.10, verapamil, HCT and unlabeled AFB1 (at concentrations used to inhibit cellular accumulation of [3 H]-AFB1) inhibit binding of [3 H]-AFB1 within 30 sec to human liver microsomal proteins. Binding did not increase when incubation continued for 10 min. Additional binding assays demonstrated that 17- β -estradiol inhibited binding of [3 H]-AFB1 to human liver microsomal protein, but probenecid, FCCP, omeprazole (OME) and corticosterone had no significant effect on binding of [3 H]-AFB1 to liver microsomal proteins (Figure 4.11).

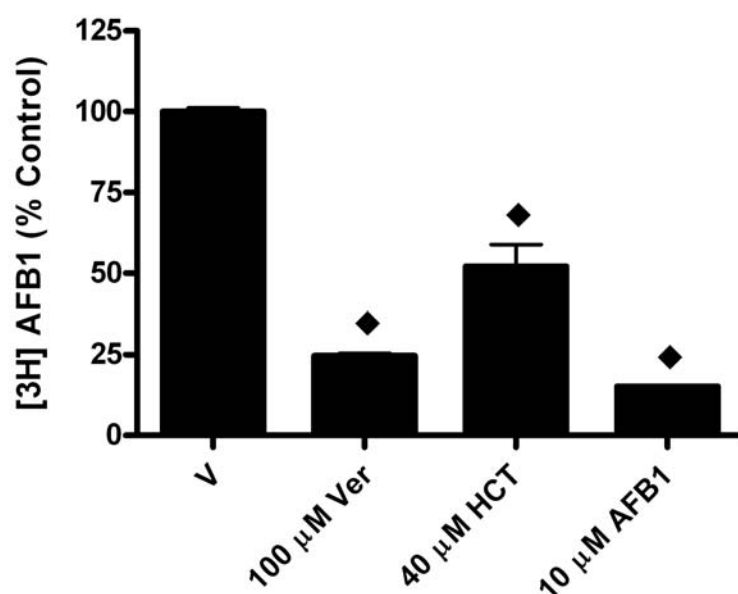


Figure 4.10 HCT, verapamil and unlabeled AFB1 decreased binding of [3 H]-AFB1 to liver microsomes. Human liver microsomes (0.1 µg protein) were incubated for 30 sec at ambient temperature with [3 H]-AFB1 + Vehicle (VEH), HCT (40 µM), VER (verapamil, 100 µM) or unlabeled AFB1 (10 µM). All treatments differ from vehicle ♦ P < 0.01.

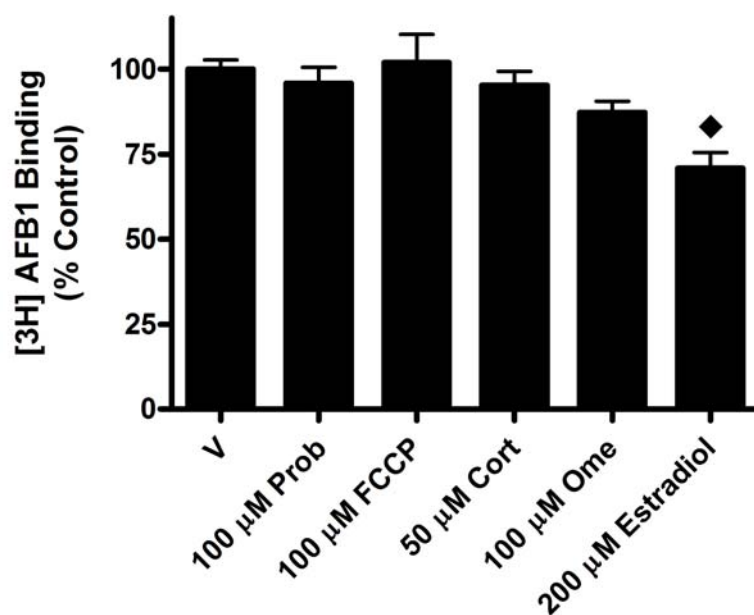


Figure 4.11 17- β -estradiol binding of [3 H]-AFB1 to human liver microsomes. Human liver microsomes (0.1 μ g protein) were incubated for 10 min at ambient temperature with [3 H]-AFB1 + Vehicle (V), probenecid (Prob), FCCP, corticosterone (Cort), omeprazole (Ome) or 17- β -estradiol (Estradiol). ♦ P < 0.01.

These findings suggested inhibition of binding to intracellular microsomal proteins accounts for most of the inhibitory effects of HCT, AFB1, and verapamil on accumulation of [3 H]-AFB1 in HepG2 cells. Absence of effects of probenecid, carbamyl cyanide 4-(trifluoromethoxy) phenylhydrazine (FCCP), and omeprazole (OME) on binding of [3 H]-AFB1 to microsomes suggested additional mechanisms modulate accumulation of [3 H]-AFB1 in HepG2 cells.

AFB1 transport by MRP-1, which is known to excrete AFB1 from cells, is enhanced by the presence of glutathione.⁵³ A small decrease in accumulation of [3 H]-AFB1 (Fig. 4.5) in the presence of a glutathione ester (GSHE) that penetrates cells was consistent with GSH-stimulation of MRP-1 mediated efflux of AFB1 conjugates.⁵³ Inhibition of [3 H]-AFB1 accumulation by 17- β -EG and estrone sulfate (substrates of several OATs, OATPs, MDR1 and MRP efflux transporters) was consistent with inhibition of the OAT/ OATP uptake transporters^{56,69} and not consistent with inhibition of efflux. Similarly, probenecid inhibits MRP1, OATs and some OATPs, inhibition of [3 H]-AFB1 accumulation was consistent with OAT or OATP-mediated uptake. These findings left open the possibility that OATs or OATPs influence AFB1 uptake and suggested that MRP1 has little effect on AFB1 transport in cultured Hep G2 cells in the absence of GSH supplements.

Inhibition with the H^+ ionophore, carbamyl cyanide 4-(trifluoromethoxy) phenylhydrazone (FCCP), which also uncouples mitochondrial oxidative phosphorylation, suggested dependence of AFB1 accumulation on membrane potential and/or pH. Failure of 100 μ M KCl, valinomycin + KCl, or nigericin to alter [3 H]-AFB1 accumulation (Fig. 4.6) suggested that changes in membrane potential did not alter AFB1 accumulation in HepG2 cells. These findings suggested the major action of FCCP on accumulation was due to its action on H^+ . Inhibition of accumulation with omeprazole, an inhibitor of H^+ ATPase (H^+ pumps) further suggested that H^+ gradients influence accumulation of [3 H]-AFB1.

Inhibition of [3 H]-AFB1 accumulation by the sulfhydryl alkylating agent N-ethylmaleimide (NEM) and reversal by dithiothrietol (DTT) suggested sulfhydryls are important for accumulation (Figure 4.6). Substitution of KBr for KCl decreased accumulation of [3 H]-AFB1 and suggested chloride ions affect AFB1 accumulation.

Although inhibition of [3 H]-AFB1 accumulation with probenecid suggested an OAT or OATP may be involved in the uptake of AFB1 in HepG2 cells, failure of PAH to inhibit AFB1 transport (Figure 4.5) eliminated most OATs and suggested OATPs, such as OATPB (also, known as OATP2B1), may take up AFB1. Gene expression of OATPs have been detected previously by others in HepG2 cells,^{58,65} and OATPB is an H^+ coupled transporter.⁷⁰ Furthermore, OATPB activity is modulated by several steroids.⁷¹ Based on evidence that extracellular acid increases OATPB activity in intestinal cells,⁶⁹ we examined effects of changes in pH of the HepG2 cell medium. In contrast to the stimulatory effects of acid on OATPB activity, Figure 4.12 indicated that extracellular

acid reduced [^3H]-AFB1 accumulation in these cells. This was our first evidence against OATPB-mediated transport of [^3H]-AFB1.

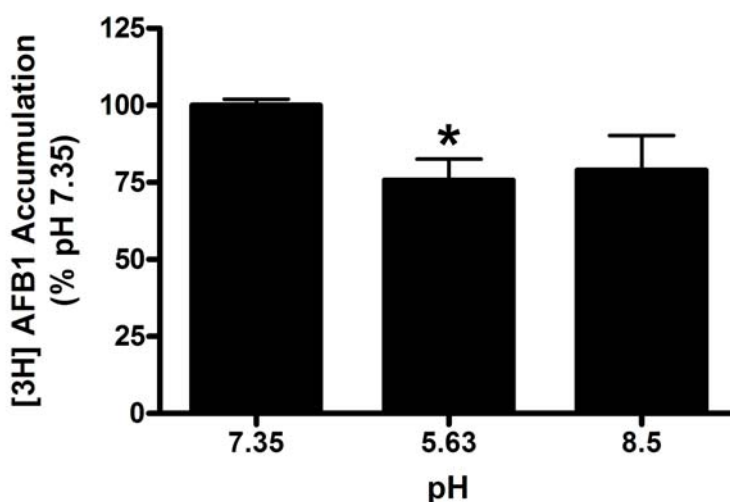


Figure 4.12 Effects of pH on accumulation of [^3H]-AFB1 in Hep G2 cells. Accumulation of [^3H]-AFB1 in HepG2 cells was measured at 10 min as described in Figure 4.1. Bars represent the mean \pm S.E. of 3-4 replicates. ;* $P < 0.05$ compared accumulation at pH 7.35.

To clarify whether OATPB affects AFB1, the accumulation of [^3H]-AFB1 was measured in Chinese hamster ovarian cells (CHO cells) transfected with the OATPB gene. Estrone sulfate is a common substrate of OATPB, and accumulation of [^3H]-ES in these cells was measured as a positive control. As demonstrated in Figure 4.13, CHO cells expressing OATPB accumulated approximately two fold more [^3H]-estrone sulfate ([^3H]-ES) than wild type cells without the gene; however, no accumulation of [^3H]-AFB1 above background levels was detected in either the wild type cells or cells expressing OATPB incubated in uptake buffer or a transport buffer typically used for OAPB (data not shown). A high concentration of HCT (100 μM) inhibited accumulation of [^3H]-ES

by approximately 15 % in both wild type and transfected cells (Figure 4.14), suggesting no specific effects of HCT on OATPB-mediated transport.

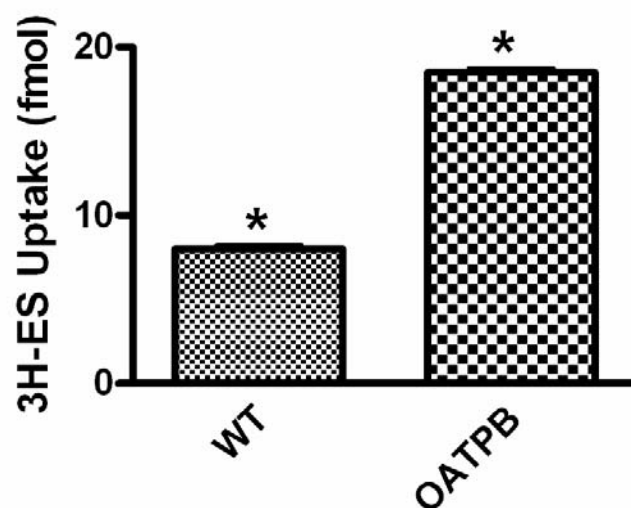


Figure 4.13 Accumulation of [³H]-ES in wild type (WT) CHO cells and CHO cells expressing OATPB. Accumulation of [³H]-estrone sulfate (ES) was measured after 10 min incubation. *P < 0.01

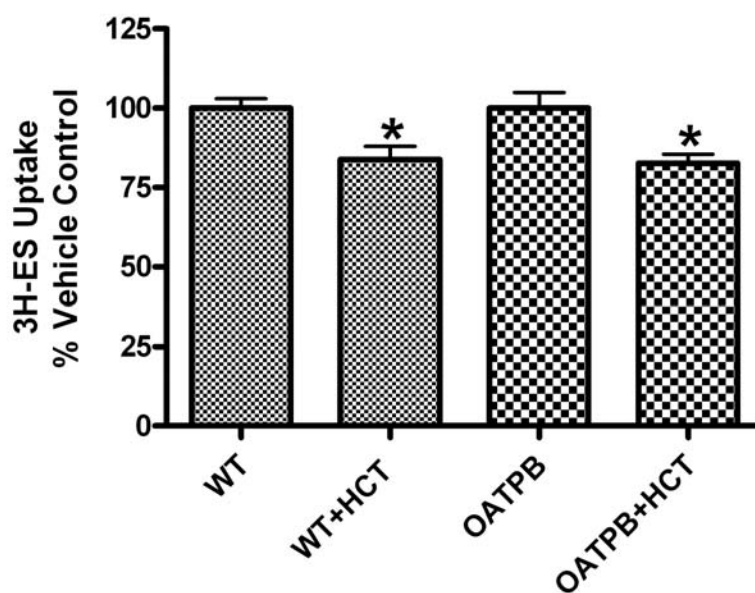


Figure 4.14 Effects of HCT on accumulation of [³H]-ES in wild type (WT) CHO cells and CHO cells expressing OATPB. Accumulation of [³H]-estrone sulfate (ES) was measured after 10 min incubation with vehicle or as 100 μ M HCT as described in Figure 4.1. *P < 0.05

In summary, these findings indicate AFB1 accumulation in HepG2 cells is saturable and suggest binding to intracellular proteins has an important effect on the rapid accumulation of AFB1 in these cells. Inhibition of AFB1 accumulation with GSHE and glucuronide is consistent with effects of the efflux transporter MRP1 on efflux of AFB1 conjugates reported by others.⁵³ The data also suggest one or more unidentified transport mechanism(s) that are proton dependent may influence accumulation of AFB1 in these cells.

Chapter 5

Preliminary Studies of Other biological actions of HCT and OHCT

5.1 Anti-inflammatory Effects of HCT on Macrophages

When we investigated the interaction between HCT and AFB1, we were also interested in other biological actions of HCT. Based on evidence that terpenes modulate immune cell production of cytokines,⁷⁴ we examined effects of HCT on production of interleukin-6 (IL-6), and tumor necrosis factor α (TNF α) by macrophages. Macrophages produce these cytokines and exhibit biological activity when the cells are activated by external invasion or chemical mediators, such as the bacterial endotoxin, lipopolysaccharide (LPS).⁷⁵

TNF α and IL-6 both are responsible for pro-inflammatory actions against infection; for example, they lead to an increase of body temperature and promote production of other pro-inflammatory cytokines,^{76, 77, 78} but IL-6 also has anti-inflammatory actions, such as suppression of TNF α expression.^{77, 79} TNF includes a family of cytokines causing cell death, but TNF α is also one of the most potent cytokines promoting inflammation.

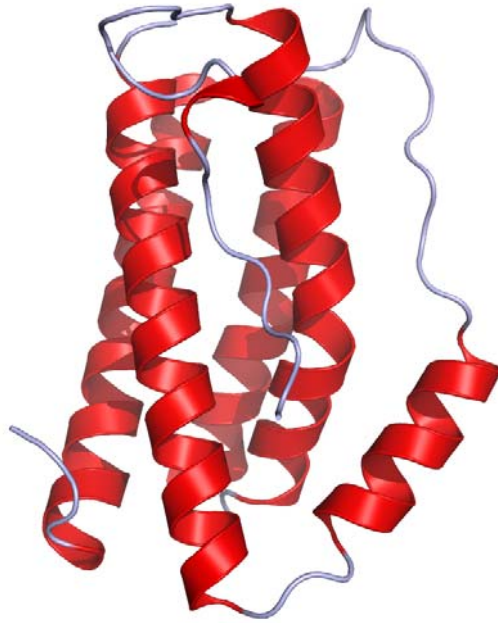


Figure 5.1 Image of human Interleukin-6

(http://upload.wikimedia.org/wikipedia/commons/e/e7/IL6_Crystal_Structure.rsh.png,

based on original data from Somers, et. al., 1997)⁸⁰

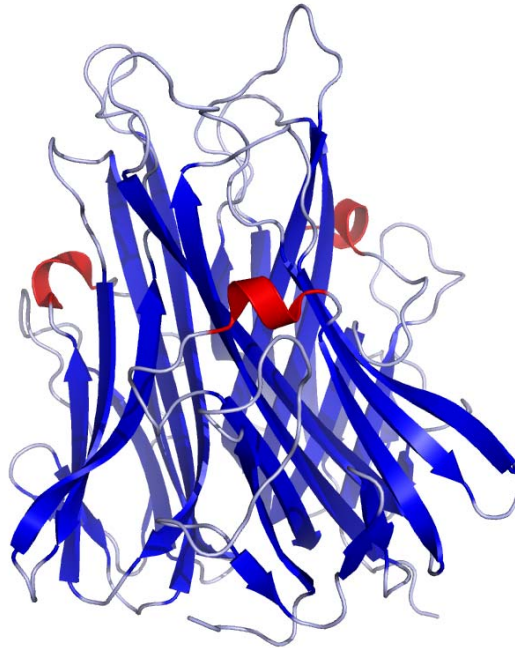


Figure 5.2 Image of human TNF α

(http://upload.wikimedia.org/wikipedia/commons/3/3b/TNFa_Crystal_Structure.rsh.png,

based on original data from Eck, et. al., 1989)⁸¹

Methods:

RAW 264.7 Macrophage Cell Line

Murine macrophages from the RAW264.7 cell line (ATTC, Rockville, MD) were cultured in RPMI (Invitrogen) supplemented with 10% heat inactivated fetal bovine serum, 1% L-glutamine, 1% non-essential amino acids, 1% minimal essential medium vitamins, 100 units/ml penicillin and 100 μ g/ml streptomycin. Cell cultures were maintained at 37 °C in 5 % CO₂ in 75 cm² tissue culture flasks (Costar Brand, Fisher Scientific, Suwanee, GA). The cultures were sub-cultured twice weekly.

Effects of HCT on LPS- induced production of cytokines

RAW264.7 macrophages (0.75×10^6) were added to each well of a 24-well tissue culture plate and incubated for 24 hrs at 37 °C in 5 % CO₂ to allow for macrophage adherence. The RAW264.7 cells doubled within 24 hours; therefore, the final concentration of all macrophages was (1.5×10^6) cells per well. The cells were washed twice with warm (37 °C) phosphate buffered saline (PBS), pH 7.4, then incubated for either 4 or 24 hrs in 500 µl of serum-free RPMI 1640 medium with and without LPS (Lipopolysaccharide, from *E. coli* – serotype 055:B5, Sigma, St. Louis, MO) and HCT or vehicle at concentrations indicated in the figure legends. Extracellular fluid was removed and centrifuged at 500 x g for 10 minutes at 4 °C to remove cellular debris, and the supernatant was frozen at -20 °C until assayed for IL-6 and TNFα. The remaining macrophage monolayer within each well was washed once with RPMI 1640 and twice with PBS. All PBS was removed, and the monolayer was lysed for subsequent measurement of total cellular protein. The cell monolayer was lysed with 150 µl of ice cold buffer containing 0.05 M Tris (pH 7.5), 0.3 M NaCl, 2 mM EDTA, 1.0 % Triton-X 100, 2 µg/ml leupeptin, 1 µg/ml aprotinin and 0.2 mM phenylmethylsulfonylfluoride. Protein concentrations of the lysates were determined with the Bio-Rad protein assay (Bio-Rad Laboratories, Hercules, CA) and read at 590 nm in the µQuant Universal Microplate reader purchased from Bio-Tek Instruments (Winooski, VT).

Measurement of cytokines

Extracellular IL-6 and TNF α concentrations were assayed with the OptEIA Multi Component ELISA Set for either Mouse IL-6 or Mouse TNF α from BD Biosciences, (San Diego, CA). The assays were performed in accordance with the manufacturer's instructions. The plates were read at 450 and 570 nm with a μ Quant Universal Microplate Spectrophotometer. Concentrations were calculated with the manufacturer's KC4 software.

Data Analyses

Analysis of variance (ANOVA) and the Neuman-Keuls test were used to compare effects of LPS and LPS + HCT or vehicle on macrophage production of TNF α and IL-6. The analyses were performed with Prism software (Graphpad, San Diego, CA). Differences were considered statistically significant at $P < 0.05$.

Results and Discussion

As shown in Fig 5.3, the amount of IL-6 and TNF α in RAW264.7 cells was increased by treatment with LPS compared to treatment with media alone. LPS acted as an endotoxin and caused a strong cell immune response, thus, leading to a significant increase of TNF α within 4 h and an increase in IL-6 within 24 h after LPS. When cells were co-treated with LPS and HCT, at 10, 20 and 40 μ M, the HCT caused a decrease of approximately 60 % IL-6 and TNF α compared to LPS only.

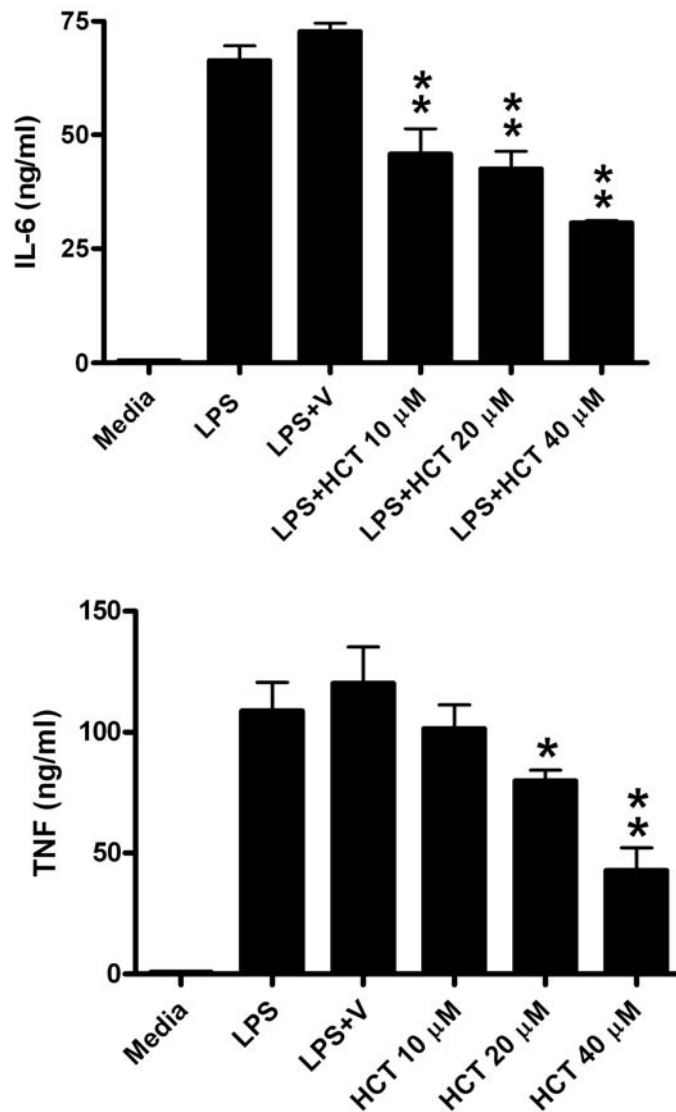


Figure 5.3 Effects of HCT on LPS-stimulated release of IL-6 and TNF α by RAW264.7 cells. Macrophages were incubated for 4 h for measurement of TNF α or for 24 h for measurement of IL-6 with media or LPS (30 ng/ml), or LPS + vehicle (V=DMSO) or the concentration of HCT shown. * $P < 0.01$ ** $P < 0.001$ compared to LPS + V.

As shown in Fig 5.4, the amount of TNF α produced by RAW264.7 cells continued to be elevated 24 h after treatment with LPS; however, the inhibitory response

to HCT was greater at 10 μ M than at 20 and 40 μ M. This may be because the higher concentrations of HCT significantly decreased IL-6, which is known to inhibit TNF α expression.⁷⁷ The lower IL-6 may have permitted a small increase in TNF α at 24 h, despite the inhibitory effects of HCT, and suggests that effects of cytokines, such as IL-6, may over-ride effects of HCT.

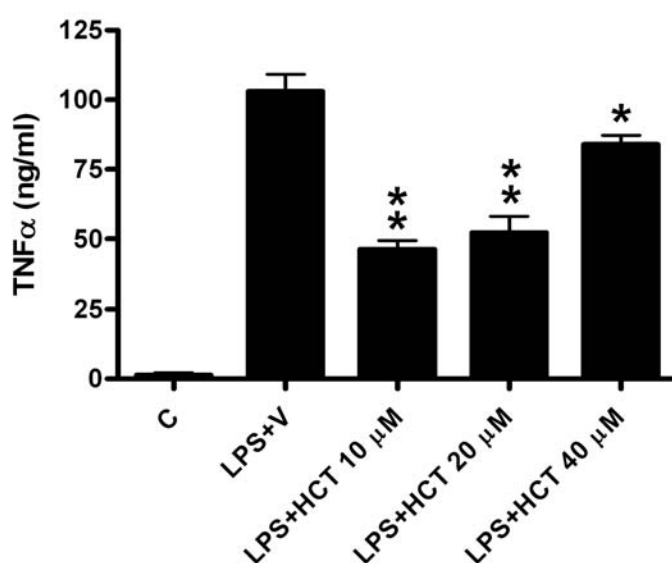


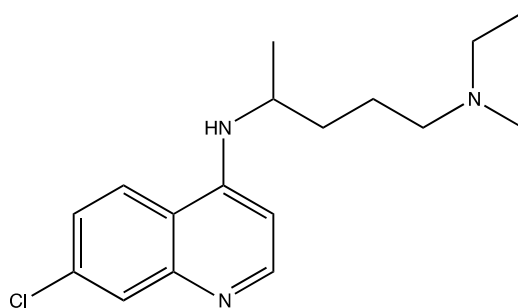
Figure 5.4 Effects of HCT on LPS-stimulated release of TNF α by RAW264.7 cells. Macrophages were incubated for 24 h with media (C) or LPS (30 ng/ml) or LPS + vehicle (V=DMSO) or LPS + the concentration of HCT shown. * P < 0.01 ** P < 0.001 compared to LPS + V

This result indicates that μ M concentrations of HCT may have an impact on LPS-stimulated IL-6 and TNF α . No effects of HCT on macrophage total cellular protein were observed (data not shown).

5.2 Biological Actions of OHCT

As described in Chapter 3, Dr. Zhou demonstrated that HCT is oxidized to OHCT in aqueous media and that both OHCT and HCT inhibit CYP P450- 3A4. Furthermore, he demonstrated that OHCT is stable in aqueous buffer for at least 72 h as determined by HPLC, and I demonstrated that OHCT exhibits no cytotoxicity at concentrations as high as 60 μ M as determined by the MTT assay.⁵⁰

While these studies were in progress, Dr. Ghislaine Mayer (Department of Biology, Virginia Commonwealth University) in collaboration with Dr. Stewart and Dr. Zhou discovered that OHCT effectively kills *Plasmodium falciparum*, a parasite that causes human malaria.⁸² They found that OHCT inhibited *in vitro* survival of all blood stages of *P. falciparum* clones, including gametocytes that are transmitted by mosquitoes and clones that are resistant to the anti-malarial drugs chloroquine and artemisinin⁸³. As shown in Table 5.1, OHCT with an IC_{50} < 40 nM was significantly more effective than chloroquine against gametocytes (Table 5.1).



Scheme 5.1 Structure of Chloroquine

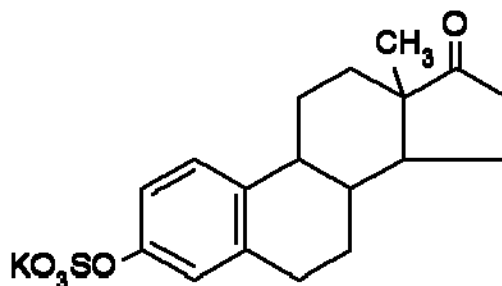
Table 5.1. OHCT (nM) inhibits growth of *P. falciparum* gametocytes*

	OHCT	Chloroquine	OHCT	Chloroquine
	(Stage I and II)	(Stage I and II)	(Stage III and IV)	(Stage III and IV)
(IC₅₀)	22 ± 3.4	394 ± 127.0	36 ± 9.0	944 ± 92.0
(IC₉₀)	174 ± 5.4	1520 ± 27.5	226 ± 49.3	2109 ± 85.2

*IC₅₀ and IC₉₀ values (nM) represent the mean ± SE of duplicate experiments, each performed in duplicate (vehicle and 8 concentrations per experiment). Stages of pure gametocyte cultures of the *P. falciparum* Dd2Nm clone were counted microscopically in 7,000 – 10,000 erythrocytes (from Mayer et al., 2009).

The protective effects of OHCT and HCT against AFB1 and the anti-malarial actions of OHCT suggested these molecules are potential new drug candidates. Cellular transport molecules are important in both uptake and removal of drugs from cells and change the bioavailability and half-life of the drugs in animals or human patients.^{84,85} If OHCT and HCT influence transporter activity and are administered to patients taking other drugs, the bioavailability of the drugs could be altered. Therefore, I began preliminary studies to examine effects of OHCT on transporter function.

To investigate effects of OHCT on activity of two of the major efflux transporter in liver cells (MRP1 and MDR1), we used radiolabeled estrone sulfate, which is a general substrate for these transporters and for organic anion transporters (OATs) and organic anion transporting polypeptides (OATPs).



Scheme 5.2 Structure of Estrone 3-sulfate potassium salt

5.3 Effects of OHCT on Cellular MDR1-mediated Efflux of AFB1 and Estrone Sulfate

As mentioned previously, inhibitory effects of HCT on AFB1 accumulation in HepG2 cells theoretically could be explained by stimulation of an efflux transporter. HepG2 cells express high levels of the efflux transporter MDR1. Although this transporter has little effect on efflux of conjugated AFB1 metabolites⁵³, it is not known if it transports unconjugated AFB1. In order to investigate the effect of OHCT on MDR1 transporter activity, we obtained MES-SA/DX5 cells over-expressing MDR1 from ATCC and studied the interactive effects of HCT and MDR1 inhibitors on accumulation of both AFB1 and the transporter substrate estrone sulfate.

Methods:

Cells: MES-SA/DX5 cells were obtained from ATCC (Manassas, VA) and maintained in 75 cm² flasks in the incubator at 37 °C with 5 % CO₂. The growth medium contained 90 % McCoy's 5a Medium Modified from ATCC (Manassas, VA) and 10 %

heat-inactivated fetal bovine serum (FBS) plus 50 Unit/mL penicillin, and 50 µg/mL streptomycin.

Transport assay: Cells were seeded in a 24 well plate at 10^6 cells / well and maintained in 1 mL of growth medium at 37° C in the incubator for 16 h prior to the transport assay. For the assay, the plate was removed from the incubator and kept at room temperature for 20 min to equilibrate. Cells were washed twice with 1 ml of sucrose/Hepes (SH) buffer which contained 0.32 M sucrose and 10 mM Hepes and adjusted to pH 7.4 with KOH. The final SH wash was removed at 1.5 min intervals, and cells were incubated for the times indicated at room temperature in 0.8 ml of uptake buffer, which contained SH supplemented with 4 mM MgSO₄, 4 mM KCl, 15 nM [³H]-AFB1, and inhibitors/substrates or vehicles. The cellular uptake was stopped by removing the uptake buffer and washing twice with SH. After the wash, cells were lysed for 5 min in 0.8 mL of 0.2 M NaOH containing 1 % sodium dodecyl sulfate. To measure cellular accumulation of radioactivity, a 400 µL aliquot of each cell lysate was added to 5 mL of Scinti-Safe Plus-50% (Fisher Scientific) and counted in the LS6000 IC scintillation counter (Beckman/Coulter). A 400 µL aliquot of uptake buffer also was counted to verify the total amount of radioactivity added to cells. For determination of background radioactivity, cells incubated for zero time in uptake buffer were included in each assay. Background radioactivity was subtracted from all measurements of cellular radioactivity.

Data Analyses: Data were analyzed with Prism version 4.00 (GraphPad Software Inc., San Diego, CA). All assays were repeated at least three times independently. Percentage values were transformed to arcsin and compared with the appropriate control by an unpaired t test.

Results and Discussion:

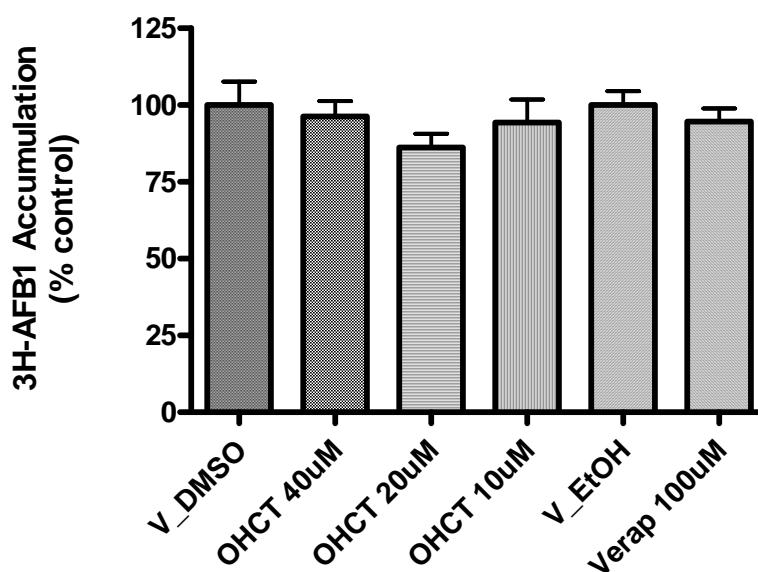


Figure 5.5 Effects of OHCT on [³H]-AFB1 accumulation. Accumulation of [³H]-AFB1 was measured at 10 min in MES-SA/DX5 cells treated with vehicle (V) or OHCT at 10, 20, 40 μ M and verapamil at 100 μ M. Bars represent mean \pm S.E. of at least 3 replicates.

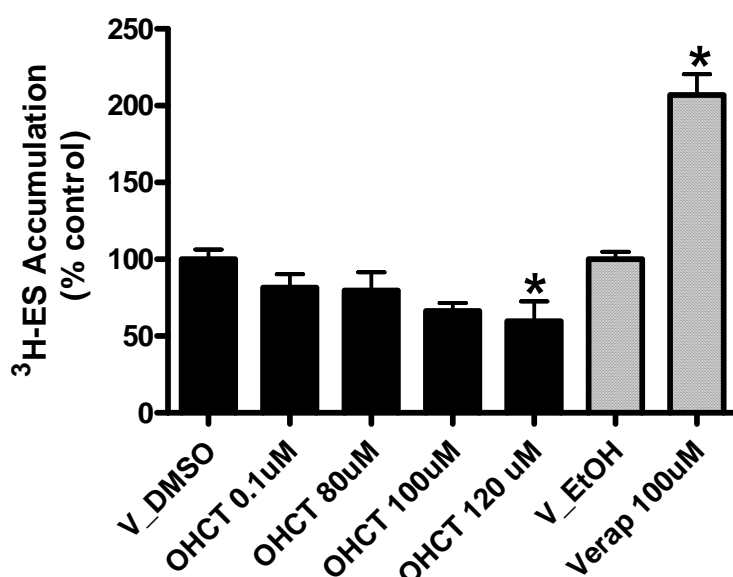


Figure 5.6 Effects of OHCT on [³H]-ES accumulation. Accumulation of [³H]-ES was measured at 10 min in MES-SA/DX5 cells treated with vehicle (V) or OHCT at 0.1, 80, 100, or 120 μ M and verapamil at 100 μ M. Bars represent mean \pm S.E. of at least 3 replicates.

As seen in Figure 5.5, neither OHCT nor 100 μ M verapamil had any effect on cellular accumulation of [³H]-AFB1, implying that AFB1 was not transported by MDR1. In order to verify MDR1 expression of MES-SA/DX5 cells and the inhibition of verapamil on MDR1, radiolabeled estrone sulfate, which is a general substrate for MDR1 transporter, was used. In Figure 5.6, it is clearly shown that 100 μ M verapamil inhibited MDR1 transporter and caused approximately 50 % increase of cellular accumulation of [³H]-ES. OHCT at a high concentration (120 μ M) appeared to stimulate MDR1-mediated efflux. Additional study is needed to verify this finding.

5.4 Preliminary studies with H69AR cells expressing MRP1

Near the end of this project, I began optimizing conditions for maintaining cells that express the efflux transporter, MRP1.

Methods:

Cells: H69AR cells were obtained from ATCC (Manassas, VA) and maintained in 75 cm² flasks in the incubator at 37 °C with 5 % CO₂. The growth medium contained 80 % RPMI-1640 from Invitrogen (Carlsbad, CA) and 20 % heat-inactivated fetal bovine serum (FBS) plus 2 mM L-glutamine, 10 mM HEPES, 1 mM sodium pyruvate, 4500 mg/L glucose, and 1500 mg/L sodium bicarbonate, 50 Unit/mL penicillin, and 50 µg/mL streptomycin.

Transport assay: In a 24 well plate, 50 µL L-poly-lysine (0.1 g/L) was added to each well to promote adherence of the cells to the wells. After 5 minutes, L-poly-lysine solution was removed and was thoroughly rinsed with sterile tissue culture grade water. The plate was then allowed to dry two hours before seeding. Cells were seeded at 0.5×10^6 cells / well and maintained in 1 mL of growth medium at 37° C in the incubator for 16 h prior to the transport assay. For the assay, the plate was removed from the incubator and kept at room temperature for 20 min to equilibrate. The medium was removed at 1.5 min intervals, and cells were incubated for the times indicated at room temperature in 0.8 ml of uptake buffer, which contained SH supplemented with 4 mM MgSO₄, 4 mM KCl, 15

nM [^3H]-AFB1, and inhibitors/substrates or vehicles. The cellular uptake was stopped by removing the uptake buffer and washing once with SH. After the wash, cells were lysed for 5 min in 0.8 mL of 0.2 M NaOH containing 1 % sodium dodecyl sulfate. To measure cellular accumulation of radioactivity, a 400 μL aliquot of each cell lysate was added to 5 mL of Scinti-Safe Plus-50% (Fisher Scientific) and counted in the LS6000 IC scintillation counter (Beckman/Coulter). A 400 μL aliquot of uptake buffer also was counted to verify the total amount of radioactivity added to cells. For determination of background radioactivity, cells incubated for zero time in uptake buffer were included in each assay. Background radioactivity was subtracted from all measurements of cellular radioactivity.

Data Analyses: Data were analyzed with Prism version 4.00 (GraphPad Software Inc., San Diego, CA). All assays were repeated at least three times independently. Percentage values were transformed to arcsin and compared with the appropriate control by an unpaired t test.

Results and Discussion:

No accumulation of [^3H]-ES could be detected in the absence of an inhibitor of MRP1-mediated efflux. As shown in Figure 5.7, accumulation of [^3H]-ES reached a maximum by 5 min. In future studies GSHE will be added to estrone sulfate to optimize efflux, and effects of OHCT on efflux will be investigated. Because of the difficulty of maintaining cells that express MRP1, I was not able to continue these studies. Further investigation will be needed to determine actions of OHCT on MRPs.

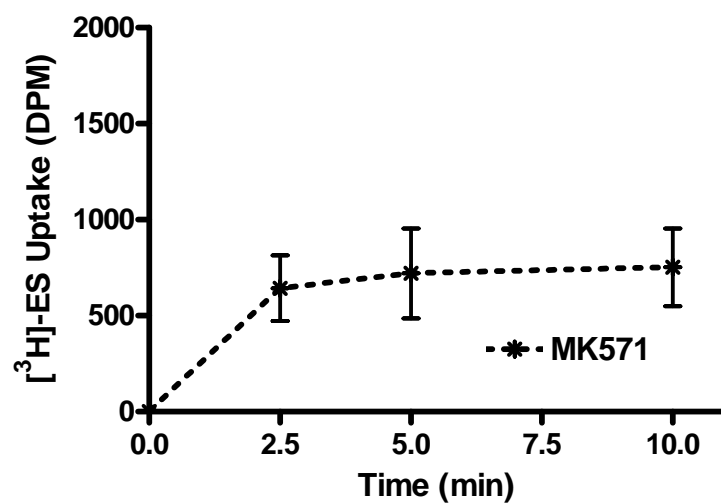


Figure. 5.7 Time-dependent accumulation of $[^3\text{H}]\text{-ES}$ by H69AR cells in the presence of the MRP1 inhibitor MK571. Cells were incubated with uptake buffer containing 15 nM $[^3\text{H}]\text{-ES}$ + 50 μM MK571 for the times indicated.

References:

1. Gershenzon, J.; Dudareva, N. "The function of terpene natural products in the natural world" *Nature Chemical Biology***2004**, 3, 408 – 414
2. Langenheim, J.H. "Higher plant terpenoids: a phytocentric overview of their ecological roles" *J. Chem. Ecol.***1994**, 20, 1223–1280
3. Dussourd, D.E.; Hoyle, A.M. "Poisoned plusiines: toxicity of milkweed latex and cardenolides to some generalist caterpillars" *Chemoecology***2000**, 10, 11–16
4. Quintana, A. et al. "Interspecific variation in terpenoid composition of defensive secretions of European *Reticulitermes* termites" *J. Chem. Ecol.***2003**, 29, 639–652
5. Fries, K. *Liebigs Ann. Chem.* **1907**, 353, 339
6. Brandon, R. L.; Sarrafzadeh, H.; Garrdner, P. D. "o-Quinonone Methide" *J. Am. Chem. Soc.***1959**, 81, 5515
7. Van De Water, R. W.; Pettus, T. R. R. "o-Quinone methides: intermediates underdeveloped and underutilized in organic synthesis" *Tetrahedron***2002**, 58, 5367-5405
8. Yang, H. J.; Chen, D.; Cui, Q.; Yuan, X. and Dou, Q. P. "Celastrol, a Triterpene Extracted from the Chinese "Thunder of God Vine," Is a Potent Proteasome Inhibitor and Suppresses Human Prostate Cancer Growth in Nude Mice" *Cancer Research*,**2006**, 66, 4758-4765
9. Chávez, H.; Estévez-Braum, A.; Ravelo, A. G.; González, A. G. "New phenolic and quinone-methide triterpenes from *Maytenus Amazonia*" *J. Nat. Prod.*,**1999**, 62, 434-436
10. Jin, H.; Hwang, B. Y.; Kim, H. S.; Lee, J. H.; Kim, Y. H.; Lee, J. J. "Antiinflammatory constituents of *Celastrus orbiculatus* inhibit the NF- κ B Activation and NO production" *J. Nat. Prod.*,**2002**, 65, 89-91
11. Marques, C. G.; Pedro, M.; Simoes, M. F. A.; Nascimento, M. S. J.; Pinto, M. M. M.; Rodriguez, B. "Effect of abietane diterpenes from *Plectranthus grandidentatus* on the growth of human cancer cell lines" *Planta Med.*,**2002**, 68, 839-840
12. Mei, S.-X.; Jiang, B.; Niu, X.-M.; Li, M.-L.; Yang, H.; Na, Z.; Lin, Z.-W.; Li, C. M.; Sun, H.-D. "Abietane diterpenoids from *Coleus Xanthanthus*" *J. Nat. Prod.*, **2002**, 65, 633-637

13. Zhou, Q.; Zuniga, M. A. "Quinone methides formation in the Cu²⁺-induced oxidation of a diterpenone catechol and concurrent damage on DNA" *Chem. Res. Toxicol.* **2005**, 18, 382-388
14. Zuniga, M. A.; Zhou, Q. "DNA Oxidative Damage by Terpene Catechols as Analogues of Natural Terpene Quinone Methide Precursors in the Presence of Cu(II) and/or NADH" *Chem. Res. Toxicol.* **2006**, 19, 828-836
15. Spartan 2002 Essential, Wavefunction Inc., Irvine CA.
16. Abbas, H. K. "Aflatoxin and food safety" Crc Press **2004**
17. Sargeant, K.; Sheridan, A.; O'Kelly, J.; Carnaghan, R. B. A. "Toxicity associated with Certain Samples of Groundnuts" *Nature*, **1961**, 192, 1096
18. Van der Zijden, A. S. M.; Blanche Koelensmid, W. A. A.; Boldingh, J.; Barrett, C. B.; Ord, W. O.; Philp, J. "Aspergillus Flavus and Turkey X Disease: Isolation in Crystalline Form of a Toxin responsible for Turkey X Disease" *Nature*, **1962**, 195, 1060 – 1062
19. <http://monographs.iarc.fr/ENG/Classification/Listagentsalphorder.pdf>
20. Ozturk, M. "p53 mutation in hepatocellular carcinoma after aflatoxin exposure" *Lancet* **1991**, 338, 1356-1369
21. Groopman, J. D; Kensler, T.W. "Role of metabolism and viruses in aflatoxin-induced liver cancer" *Toxicol. Appl. Pharmacol.* **2005**, 206, 131-137
22. Farmer, B. P; Sharma, A. R. "Biological Relevance of Adduct Detection to the Chemoprevention of Cancer" *Clin. Cancer Res.* **2004**, 10, 4901-4912
23. Verma, A; Judah, J. D; Eaton, L. D; Neal, E. G. "Metabolism and Toxicity of Aflatoxins M1 and B1 in human derived in vitro systems" *Toxic and Appl. Pharm.* **1998**, 151, 152-158
24. Ueng, Y.-F.; Shimada, T.; Yamazaki, H.; Guengerich, F. P.; "Oxidation of aflatoxin B1 by bacterial recombinant human cytochrome P450 enzymes", *Chem. Res. Toxicol.* **1995**, 8, 218–225.
25. Guengerich, F. P.; Johnson, W. W.; Shimada, T.; Ueng, Y. F.; Yamazaki, H.; Langouet, S.; "Activation and detoxication of aflatoxin B1", *Mutation Research* **1998**, 402, 121–128
26. Smela, M. E.; Currier, S. S.; Bailey, E. A.; Essigmann, J. M. "The chemistry and biology of aflatoxin B1: from mutational spectrometry to carcinogenesis" *Carcinogenesis*, **2001**, 22(4), 535-545

27. Johnson, W. W.; Guengerich, F. P. "Reaction of aflatoxin B₁ exo-8,9-epoxide with DNA: kinetic analysis of covalent binding and DNA-induced hydrolysis", *Proc. Natl. Acad. Sci. U.S.A.* **1997**, 94, 6121–6125.
28. Ortiz de Montellano, P. R. "Cytochrome P450: Structure, mechanism and biochemistry" *Plenum Press, New York and London*, **1995**
29. Poulos, T. L.; Finzel, B. C.; Howard, A. J. "High-resolution crystal structure of cytochrome P450cam" *J. Mol. Biol.* **1987**, 195, 687-700
30. Ravichandran, K. G.; Boddupali, S. S.; Hasermann, C. A.; Peterson, J. A.; Deisenhofer J. "Crystal structure of hemoprotein domain of P450BM-3, a prototype for microsomal P450's" *Science*, **1993**, 261, 731-736
31. Hayaishi, O.; Katagiri, M.; Rothberg, S. "Mechanism of the pyrochatecase reaction" *J. Am. Chem. Soc.* **1955**, 77, 5450-5451
32. Meunier, B.; de Visser, S. P.; Shaik, S. "Mechanism of Oxidation Reactions Catalyzed by Cytochrome P450 Enzymes". *Chem. Rev.* **2004**, 104, 3947 – 3980
33. Beaune, P.; Dansette, P.; Flinois, J. P.; Columelli, S.; Mansuy, D.; Leroux, J. P. "Partial purification of human liver cytochrome P 450" *Biophys. Res. Commun.* **1979**, 88, 826-832
34. Wang, P.; Mason, P. S.; Guengerich, F. P. "Purification of human liver cytochrome P-450 and comparison to the enzyme isolated from rat liver" *Arch. Biochem. Biophys.* **1980**, 99, 206-219
35. Wang, P. P.; Beaune, P.; Kaminsky, L. S.; Dannan, G. A.; Kadlubar, F. F.; Larrey, D.; Guengerich, F. P. "Purification and characterization of six cytochrome P-450 isozymes from human liver microsomes" *Biochemistry* **1983**, 22, 5375-5383
36. Rendic, S. "Summary of information on human CYP enzymes: Human. P450 substrates and inhibitors" *Drug Metab. Rev.* **2002**, 34, 69–448
37. Evans, W. E.; Relling, M. V. "Pharmacogenomics: Translating functional genomics into rational therapeutics" *Science* **1999**, 286, 487-491
38. Zhang, B. C., Zhu, Y. R., Wang, J. B., Wu, Y., Zhang, Q. N., Qian, G. S., Kuang, S. Y., Li, Y. F., Fang, X., Yu, L. Y., De Flora, S., Jacobson, L. P., Zarba, A., Egner, P. A., He, X., Wang, J. S., Chen, B., Enger, C. L., Davidson, N. E., Gordon, G. B., Gorman, M. B., Prochaska, H. J., Groopman, J. D., Munoz, A., and Kensler, T. W. "Oltipraz chemoprevention trial in Qidong, Jiangsu province, People's Republic of China" *J. Cell. Biochem. Suppl.* **1997**, 28-29, 166-173

39. Jacobson, L. P., Zhang, B. C., Zhu, Y. R., Wang, J. B., Wu, Y., Zhang, Q. N., Yu, L. Y., Qian, G. S., Kuang, S. Y., Li, Y. F., Fang, X., Zarba, A., Chen, B., Enger, C. L., Davidson, N. E., Gorman, M. B., Gordon, G. B., Prochaska, H. J., Egner, P. A., Groopman, J. D., Munoz, A., Helzlsouer, K. J., and Kensler, T. W. "Oltipraz chemoprevention trial in Qidong, People's Republic of China: study design and clinical outcomes" *Cancer Epidemiol., Biomarkers PreV.* **1997**, 6, 257-265
40. Egner, P. A., Wang, J. B., Zhu, Y. R., Zhang, B. C., Wu, Y., Zhang, Q. N., Qian, G. S., Kuang, S. Y., Gange, S. J., Jacobson, L. P., Helzlsouer, K. J., Bailey, G. S., Groopman, J. D., and Kensler, T. W. "Chlorophyllin intervention reduces aflatoxin-DNA adducts in individuals at high risk for liver cancer" *Proc. Natl. Acad. Sci. U.S.A.* **2001**, 98, 14601-14606
41. Egner, P. A., Stansbury, K. H., Snyder, E. P., Rogers, M. E., Hintz, P. A., and Kensler, T. W. "Identification and characterization of chlorin e4 ethyl ester in sera of individuals participating in the chlorophyllin chemoprevention trial" *Chem. Res. Toxicol.* **2000**, 13, 900-906
42. Guengerich, F.P.; Chun, Y.-J.; Kim, D; Gillam, E.M.J.; Shimadda, T. "Cytochrome P450 1B1: a target for inhibition in anticarcinogenesis strategies" *Mut. Res.*, **2003**, 523-524, 173-182
43. McFadyen, M.C.; Melvin, W.T.; Murray, G.I. "Cytochrome P450 enzymes: Novel options for cancer therapeutics" *Mol. Cancer Ther.*, **2004**, 3, 363-371
44. Chun, Y.-J.; Kim, S. "Discovery of cytochrome P450 inhibitors as new promising anti-cancer agents". *Med. Res. Rev.* **2003**, 23, 657-668
45. Montero, R.; Serrano, L.; Da'vila, V.M.; Ito, A.; Plancarte, A. "Infection of rats with *Taenia taeniformis* metacestodes increases hepatic CYP450, induces the activity of CYP1A1, CYP2B1 and COH isoforms and increases the genotoxicity of the procarcinogens benzo[a]pyrene, cyclophosphamide and aflatoxin B1" *Mutagenesis*, **2003**, 18, 211-216
46. Bolton, J. L.; Pisha, E.; Zhang, F.; Qiu, S. "Role of quinoids in estrogen carcinogenesis" *Chem. Res. Toxicol.* **1998**, 10, 1113-1127
47. Wood, E.; Broekman, M.J.; Kirley, T.L.; Diani-Moore, S.; Tickner, M.; Drosopoulos, J.H.F.; Islam, N.; Park, J.I.; Marus, A.J.; Rifkind, A.B. "Cell-type specific of ectonucleotidase expression and upregulation by 2,3,7,8-tetrachlorodibenzo-p-dioxin" *Arch. Biochem. Biophys.*, **2004**, 407, 49-62
48. Ueng, Y.-F.; Kuwabara, T.; Chun, Y.-J.; and Guengerich, F. P. "Cooperativity in oxidation catalyzed by cytochrome P450 3A4". *Biochem.* **1997**, 36, 370-381

49. Zhou, Q.; Xie, H.; Zhang, L.; Stewart, J. K.; Gu, X. X.; and Ryan, J. J. "cis-Terpenones as an Effective Chemopreventive Agent against Aflatoxin B1 Induced Cytotoxicity and TCDD-induced P450 1A/B activity in HepG2 Cells" *Chem. Res. Toxicol.* **2006**, 19, 1415-1419
50. Zhou Q.; Zhang L.; Zuniga M. A.; Tombes R. M.; Stewart J. K. "Mixed Inhibition of P450 3A4 as a Chemoprotective Mechanism against Aflatoxin B1-Induced Cytotoxicity with cis-Terpenones" *Chem. Res. Toxicol.* **2008**, 21(3), 732-738
51. Ewaskiewicz, J. I., Devlin, T. M., and Ch'ih, J. J. "The in vivo disposition of aflatoxin B1 in rat liver" *Biochem. Biophys. Res. Commun.* **1991**, 179, 1095-1100
52. Müller, N. and Petzinger, E. "Hepatocellular uptake of aflatoxin B1 by non-ionic diffusion. Inhibition of bile acid transport by interference with membrane lipids" *Biochim. Biophys. Acta* **1988**, 938, 334-344
53. Loe, D. W., Stewart, R. K., Massey, T. E., Deeley, R. G., and Cole, S. P. "ATP-dependent transport of aflatoxin B1 and its glutathione conjugates by the product of the multidrug resistance protein (MRP) gene" *Mol. Pharmacol.* **1997**, 51, 1034-1041
54. Ch'ih, J. J. and Devlin, T. M. "The distribution and intracellular translocation of aflatoxin B1 in isolated hepatocytes" *Biochem. Biophys. Res. Commun.* **1984**, 122, 1-8
55. Guengerich, F. P. "Cytochrome P450 oxidations in the generation of reactive electrophiles: epoxidation and related reactions" *Arch. Biochem. Biophys.* **2003**, 409, 59-71
56. Deeley, R. G. and Cole, S. P. "Substrate recognition and transport by multidrug resistance protein 1 (ABCC1)" *FEBS Lett.* **2006**, 580, 1103-1111
57. Finn, J. P., Merickel A. and Edwards R.H. "Analysis of neurotransmitter transport into secretory vesicles. In: Methods in Enzymology, Vol. 296. Neurotransmitter Transporters, edited by Amara S. G." New York, NY: Academic Press, **1998**, 144-162
58. Lee, T. K., Hammond, C.L., and Ballatori, N. "Intracellular glutathione regulates taurocholate transport in HepG2 Cells" *Toxicol Applied Pharmacol.* **2001**, 174, 207-215
59. Roelofsen, H., Vos, T.A., Schippers, I.J., Kuipers, F., Koning, H., Moshage, H., Jansen, P.L., Müller, M. "Increased levels of the multidrug resistance protein in lateral membranes of proliferating hepatocyte-derived cells" *Gastroenterology* **1997**, 112(2), 511-21

60. Schrenk, D., Baus, P.R., Ermel, N., Klein, C., Vorderstemann, B., Kauffmann, H.M. "Up-regulation of transporters of the MRP family by drugs and toxins" *Toxicol Lett.***2001**, 120(1-3), 51-7
61. Rius, M., Nies, A.T., Hummel-Eisenbeiss, J., Jedlitschky, G., Keppler, D. "Cotransport of reduced glutathione with bile salts by MRP4 (ABCC4) localized to the basolateral hepatocyte membrane" *Hepatology***2003**38(2), 374-84
62. Lee, G., Piquette-Miller, M. "Cytokines alter the expression and activity of the multidrug resistance transporters in human hepatoma cell lines; analysis using RT-PCR and cDNA microarrays" *J Pharm Sci.***2003**, 92(11), 2152-63
63. Smitherman, P.K., Townsend, A.J., Kute, T.E., Morrow, C.S. "Role of multidrug resistance protein 2 (MRP2, ABCC2) in alkylating agent detoxification: MRP2 potentiates glutathione S-transferase A1-1-mediated resistance to chlorambucil cytotoxicity" *J Pharmacol Exp Ther.***2004**,308(1), 260-7
64. Dabrowska, M., Sirotnak, F.M. "Regulation of transcription of the human MRP7 gene. Characteristics of the basal promoter and identification of tumor-derived transcripts encoding additional 5' end heterogeneity" *Gene.* **2004**, 27(341), 129-39
65. Le Vee M., Jigorel, E., Glaise, D., Gripon, P., Guguen-Guillouzo, C., Fardel, O. "Functional expression of sinusoidal and canalicular hepatic drug transporters in the differentiated human hepatoma HepaRG cell line" *Eur J Pharm Sci.***2006**, 28(1-2), 109-17
66. Manov, I., Bashenko, Y., Hirsh, M., Iancu, T.C. "Involvement of the multidrug resistance P-glycoprotein in acetaminophen-induced toxicity in hepatoma-derived HepG2 and Hep3B cells" *Basic Clin Pharmacol Toxicol.* **2006**, 99(3), 213-24
67. Li, L., Xu, J., Min, T., Huang, W. "Up-regulation of P-glycoprotein expression by catalase via JNK activation in HepG2 cells" *Redox Rep.* **2006**, 11(4), 173-8
68. Frempong-Manso, E., Raygada, J.L., DeMarco, C.E., Seo, S.M., Kaatz, G.W. "Inability of a reserpine-based screen to identify strains overexpressing efflux pump genes in clinical isolates of *Staphylococcus aureus*" *Int J Antimicrob Agents.* **2009**, 33(4), 360-3
69. Kobayashi, D., Nozawa, T., Imai, K., Nezu, J., Tsuji, A., Tamai, I. "Involvement of human organic anion transporting polypeptide OATP-B (SLC21A9) in pH-dependent transport across intestinal apical membrane" *J. Pharmacol Exp Ther.***2003**, 306(2), 703-8
70. Thwaites, D.T., Anderson, C.M. " H^+ coupled nutrient, micronutrient and drug transporters in the mammalian small intestine" *Exp Physiol.* **2007** 92(4), 603-19

71. Grube, M., Köck, K., Karner, S., Reuther, S., Ritter, C. A., Jedlitschky, G., Kroemer, H. K. "Modification of OATP2B1-mediated transport by steroid hormones" *Mol Pharmacol.* **2006**, 70(5), 1735-41
72. Le Vee M., Jigorel E., Glaise D., Gripon P., Guguen-Guillouzo C., Fardel O. "Functional expression of sinusoidal and canalicular hepatic drug transporters in the differentiated human hepatoma HepaRG cell line" *Eur J Pharm Sci.* **2006**, 28, 109-17
73. Smitherman P. K., Townsend A. J., Kute T. E., Morrow C. S. "Role of multidrug resistance protein 2 (MRP2, ABCC2) in alkylating agent detoxification: MRP2 potentiates glutathione S-transferase A1-1-mediated resistance to chlorambucil cytotoxicity" *J Pharmacol Exp Ther.* **2004**, 308, 260-7
74. Calou, I. B.; Sousa, D. I.; Cunha, G. M.; Brito, G. A.; Silveira, E. R.; Rao, V. S.; Santos, F. A.; "Topically applied diterpenoids from *Egletes viscosa* (Asteraceae) attenuate the dermal inflammation in mouse ear induced by tetradecanoylphorbol 13-acetate- and oxazolone" *Biol Pharm Bull.* **2008**, 8, 1511-6
75. Dinarello, C. A. "The interleukin-1 family: 10 years of discovery" *The FASEB Journal*, **1994**, 8, 1314-1325
76. Ahmed, S. T.; and Ivashkiv, L. B.; "Inhibition of IL-6 and IL-10 Signaling and Stat Activation by Inflammatory and Stress Pathways" *J Immunol* **2000**, 165, 5227-5237
77. Janeway, C. A.; Travers, P.; Walport, M.; Schlomchik, M. J.; "The Immune System in Health and Disease" *Immunobiology* **2001**, Garland Pub, New York
78. Papanicolaou, D. A.; Wilder, R. L.; Manolagas, S. C. Chrousos, G. P.; "The Pathophysiological Roles of Interleukin-6 in Human Disease". *Annals of Internal Medicine* **1998**, 128, 127-137
79. Straub, R. H.; Westermann, J.; Scholmerich, J.; Falk, W.; "Dialogue between the CNS and the immune system in lymphoid organs" *Immunology Today* **1998**, 19, 409-413
80. Somers, W., Stahl, M., Seehra, J.S. "A crystal structure of interleukin 6: implications for a novel mode of receptor dimerization and signaling" *EMBO J.* **1997**, 16, 989-997
81. Eck, M.J., Sprang, S.R. "The structure of tumor necrosis factor-alpha at 2.6 Å resolution. Implications for receptor binding" *J. Biol. Chem.* **1989**, 264, 17595-17605

82. Mayer, G., Bruce, M., Kochurova, O., Stewart, J. K., Zhou, Q. "Anti-malarial activity of a cis-terpenone" *Malaria J* **2009**, 139 -142.
83. Hunt P., Afonso A., Creasey A., Culleton R., Sidhu A. B., Logan J., Valderramos S. G., McNae I., Cheesman S., do Rosario V., Carter R., Fidock D. A., Cravo P. "Gene encoding a deubiquitinating enzyme is mutated in artesunate- and chloroquine-resistant rodent malaria parasites" *Mol Microbiol.* **2007**, 65:27-40
84. Li P., Wang G. J., Robertson T. A., Roberts M. S. "Liver transporters in hepatic drug disposition: an update" *Curr Drug Metab.* **2009**, 10, 482-98
85. Ballatori N., Krance S. M., Marchan R., Hammond C. L. "Plasma membrane glutathione transporters and their roles in cell physiology and pathophysiology" *Mol Aspects Med.* **2009**, 30, 13-28.

VITA

Lin Zhang was born on November 4, 1973, in Tianjin, China, and is a Chinese citizen. He graduated from Yaohua High School, Tianjin, China in 1992. He received his Bachelor of Sciences in Chemistry from Nankai University, Tianjin, China in 1996 and his Master of Science in Polymer from Nankai University, Tianjin, China in 1999. He is the author of two publications.